Xuan-Liang Unified Field Theory: From Multi-Velocity Xuan-Liang Construction to Cosmology and Astrophysical Tests

Jianchao Hou *

Posted Date: 28 February 2026

doi: 10.20944/preprints202602.1996.v1

Keywords: Xuan-Liang; modified gravity; dark matter; dark energy; galaxy rotation curves; unified field theory; cosmology

 doi:10.20944/preprints202602.1996.v1

Article

Xuan-Liang Unified Field Theory: From Multi-Velocity Xuan-Liang Construction to Cosmology and Astrophysical Tests

Jianchao Hou

Independent Researcher, China; 517282455@qq.com

Abstract

Modern physics rests on two pillars: general relativity and quantum field theory. However, they are not yet unified, and observations of dark matter and dark energy suggest shortcomings in existing theories. This paper presents a comprehensive reconstruction and extension of the Xuan-Liang unified field theory. Starting from first principles, we define Xuan-Liang as the line integral of power along a path, filling the geometric hierarchy of physical quantities (mass, momentum, kinetic energy, Xuan-Liang). A key advancement is the generalization of the Xuan-Liang concept to multi-velocity components, i.e., the Xuan-Liang of a complex system (such as a galaxy) is the product of its various characteristic velocities (e.g., rotation, revolution, bulk motion). This naturally leads to a modified Newtonian potential of the Yukawa form: $\Phi(r) = -\frac{GM}{r}[1 + \delta(1 - e^{-r/\lambda})]$, where the coupling strength δ and characteristic scale λ arise from multi-velocity coupling. Based on the action principle, we rigorously derive the unified field equations, demonstrating their self-consistency and their reduction to general relativity, Newtonian gravity, and cosmology. The theory's explanatory power is demonstrated through applications: (i) it perfectly fits galaxy rotation curves from dwarf galaxies to the Milky Way and Andromeda, spanning a huge mass range, without requiring dark matter particles; (ii) it provides a dynamical dark energy model whose energy density smoothly transitions from matter-like behavior ($w \approx 0$) at high densities to cosmological-constant-like behavior ($w \approx -1$) at low densities, consistent with cosmic acceleration; (iii) it predicts testable modifications to black hole thermodynamics and strong-field gravity, including changes in black hole shadows and gravitational wave signals. The multi-velocity construction not only resolves the theoretical inadequacy of single-velocity Xuan-Liang in explaining galactic dynamics but also builds a mathematically self-consistent, experimentally testable unified framework. Finally, we discuss prospects for quantization and a roadmap for future observational tests.

Keywords: Xuan-Liang; modified gravity; dark matter; dark energy; galaxy rotation curves; unified field theory; cosmology

PACS: 98.80.-k, 95.35.+d, 95.36.+x, 04.50.-h, 04.60.-m

1. Introduction

Modern physics is built upon two pillars: general relativity and quantum field theory. General relativity successfully describes the connection between gravity and spacetime geometry, while quantum field theory perfectly explains the electromagnetic, weak, and strong interactions. However, efforts to incorporate gravity into a quantum framework have not yet succeeded, and cosmological observations revealing dark matter and dark energy suggest shortcomings in existing theories.

This paper proposes a novel unified field theory framework—Xuan-Liang unified field theory. Starting from fundamental kinematic quantities, we introduce a new physical quantity, "Xuan-Liang", defined as $X = \frac{1}{3}mv^3$, filling the geometric sequence after mass, momentum, and kinetic energy. By geometrizing Xuan-Liang as a differential form and constructing a unified action incorporating curvature coupling and Xuan-Liang dynamics, we derive a set of self-consistent unified field equations.

 doi:10.20944/preprints202602.1996.v1

The main contributions of this paper include:

1. Proposing a hierarchical definition system for the Xuan-Liang concept, allowing flexible construction of differential forms for different physical contexts.
2. Establishing a rigorous differential geometric definition, correcting mathematical issues in the original definition.
3. Deriving the unified equations in detail, including both integral and differential forms, ensuring their equivalence.
4. Systematically proving the reduction to classical theories (general relativity, Newtonian gravity, cosmology), ensuring consistency of the reduction.
5. Presenting application examples in dark matter, dark energy, black hole physics, and the early universe.
6. Providing testable theoretical predictions and an experimental roadmap.

2. Basic Definition and Geometric Meaning of Xuan-Liang

2.1. Algebraic Definition and Physical Origin of Xuan-Liang

For an object of mass m and velocity v, its Xuan-Liang X is defined as:

$$X = \frac{1}{3}mv^3 \tag{1}$$

Its dimension is $[M][L]^3[T]^{-3}$, filling the geometric gap in the sequence of physical quantities. The term "Xuan-Liang" is derived from the Chinese classics *I Ching* ("heaven is dark, earth is yellow") and *Tao Te Ching* ("the mystery of mysteries, the gate of all wonders"), signifying a profound and fundamental property of motion.

Remark 1. *The coefficient* $1/3$ *is a natural consequence of the geometric hierarchy. In the path integral of uniformly accelerated linear motion, this coefficient appears naturally, ensuring that Xuan-Liang and kinetic energy* $\frac{1}{2}mv^2$ *form a complete geometric sequence. Consider uniformly accelerated motion* $v(t) = at$*; the power* $P = mav$*, integrated along the path:*

$$\int Pdl = \int mav \cdot vdt = ma^2 \int t^2 dt = \frac{1}{3}ma^3t^3 = \frac{1}{3}mv^3$$

2.2. Geometric Hierarchy: From Mass to Xuan-Liang

The physical quantities describing the state of motion in classical mechanics exhibit a clear geometric hierarchy:

Table 1. Geometric hierarchy of physical quantities

Order	Quantity	Expression	Dimension	Geometric interpretation
0	Mass	m	$[M]$	Point attribute: existence
1	Momentum	$m\vec{v}$	$[M][L][T]^{-1}$	Line attribute: directed motion
2	Kinetic energy	$\frac{1}{2}mv^2$	$[M][L]^2[T]^{-2}$	Surface attribute: intensity of motion
3	Xuan-Liang	$\frac{1}{3}mv^3$	$[M][L]^3[T]^{-3}$	Volume attribute: accumulation of energy flow

This sequence reveals an intrinsic symmetry of physical quantities: m (scalar, order 0) $\rightarrow mv$ (vector, order 1) $\rightarrow \frac{1}{2}mv^2$ (scalar, order 2) $\rightarrow \frac{1}{3}mv^3$ (pseudoscalar, order 3).

2.3. Path-Integral Definition of Xuan-Liang

In physics, the effect of a force on the motion of an object is manifested through accumulation over space—work:

$$W = \int_C \vec{F} \cdot d\vec{x} = \Delta E_k, \quad E_k = \frac{1}{2}mv^2 \tag{2}$$

 doi:10.20944/preprints202602.1996.v1

The instantaneous rate of energy change is power:

$$P = \frac{dE_k}{dt} = \vec{F} \cdot \vec{v} \tag{3}$$

Xuan-Liang is defined as the line integral of power along the path of motion:

Definition 1 (Xuan-Liang: path integral of power)**.** *Xuan-Liang X is defined as the line integral of power P along the motion path C:*

$$\boxed{X := \oint_C P\, dl = \oint_C \frac{dE_k}{dt}\, dl} \tag{4}$$

where dl is the line element of the path. This definition gives X a clear geometric meaning: it measures the total "deposition" of the action that changes kinetic energy along the entire trajectory.

For uniformly accelerated linear motion with acceleration a and initial velocity zero, we have $v = at$, $P = ma^2t$, $dl = vdt = atdt$, and substituting into the integral gives:

$$X = \int_0^T ma^2t \cdot atdt = ma^3 \int_0^T t^2 dt = \frac{1}{3}m(aT)^3 = \frac{1}{3}mv^3,$$

consistent with the algebraic definition.

3. Hierarchical Definition System of the Xuan-Liang Concept

In the history of physics, many concepts have evolved from fixed forms to context-dependent ones. For example:

- Energy: from mechanical energy to thermal, electrical, chemical, etc.
- Momentum: from classical momentum to relativistic momentum, quantum momentum operator.
- Field: from classical fields to quantum fields, from scalar fields to spinor fields, gauge fields.

Based on this historical perspective, we propose: **The differential form of Xuan-Liang can be flexibly constructed according to the needs of specific physical problems**. This flexibility is not a weakness of the theory but an advantage for adapting to different physical scales and contexts.

Definition 2 (Hierarchical system of the Xuan-Liang concept)**.** *The Xuan-Liang concept can be divided into the following levels according to physical context:*

1. ***Classical particle level**: $X = \frac{1}{3}mv^3$ (scalar)*
2. ***Continuum level**: $\mathbf{X} = \frac{1}{3}\rho v^3 \mathbf{n}$ (vector field, $\mathbf{n}$ is direction)*
3. ***Multiple motion modes combination level**: $X = \kappa m(v_1 v_2 v_3)$ (product of multiple velocities)*
4. ***Relativistic continuum level**: $X^\mu = \frac{1}{3}\rho_0 c^2(\gamma^3 - \gamma)u^\mu$ (four-vector)*
5. ***Differential geometry level**: $\mathbb{X} = \kappa\rho_0\gamma^3 v^2 \star u$ (differential form)*
6. ***Quantum level**: $\hat{X} = \frac{1}{3}m\hat{v}^3$ (operator)*
7. ***Quantum field theory level**: $\mathcal{X}(x) = \psi^\dagger\gamma^0(\frac{1}{3}v^3)\psi$ (field operator)*

Each level corresponds to different physical situations and approximations, from simple to complex, from concrete to abstract.

3.1. Multi-Velocity Combination Definition of Xuan-Liang

In many physical systems, an object participates in multiple modes of motion simultaneously. For example:

- **Electron in an atom**: simultaneously has
  1. Translational velocity of the whole atom v_{trans}
  2. Orbital velocity around the nucleus v_{orbit}

 doi:10.20944/preprints202602.1996.v1

3. Spin motion (equivalent velocity) v_{spin}

- **Earth's motion**: simultaneously has
  1. Rotational velocity v_{rot}
  2. Revolutionary velocity v_{rev}
  3. Velocity of the Solar System around the Galactic center v_{gal}

For such systems, Xuan-Liang can be naturally extended to the form of a product of multiple velocities:

Definition 3 (Multi-velocity Xuan-Liang)**.** *For a system with n independent motion modes, Xuan-Liang is defined as:*

$$X = \kappa m \prod_{i=1}^{n} v_i^{\alpha_i} \tag{5}$$

where:

- v_i*: characteristic velocity of the i-th motion mode*
- α_i*: exponent of the i-th velocity, satisfying* $\sum_{i=1}^{n} \alpha_i = 3$
- κ*: normalization coefficient determined by the specific geometric structure of motion*

3.1.1. Special Case Analysis

Example 1 (Equal-weight product of three velocities)**.** *When the system has three equally weighted motion modes, take* $\alpha_i = 1$*, then:*

$$X = \kappa m(v_1 v_2 v_3) \tag{6}$$

For the electron:

$$X_e = \kappa_e m_e (v_{trans} \cdot v_{orbit} \cdot v_{spin})$$

For the Earth:

$$X_\oplus = \kappa_\oplus M_\oplus (v_{rot} \cdot v_{rev} \cdot v_{gal})$$

Example 2 (Significance of coefficient variation)**.** *The variation of* κ *reflects geometric features in different physical contexts:*

1. ***Classical uniformly accelerated motion****:* $\kappa = \frac{1}{3}$*, from path integral*
2. ***Rotational motion****:* $\kappa = \frac{2}{3\pi}$*, from geometric factor of circular motion*
3. ***Quantum systems****:* $\kappa = \frac{\hbar}{m\lambda_c}$*, introducing Compton wavelength* λ_c
4. ***Cosmological scales****:* $\kappa = \frac{H_0^2}{c^2}$*, related to the Hubble constant*

3.2. Physical Interpretation

The definition of multi-velocity Xuan-Liang has profound physical implications:

1. **Coupling of motion modes**: The product of different velocities reflects interrelations between motion modes.
2. **Hierarchical structure**: v_1 (micro) $\times$ v_2 (meso) $\times$ v_3 (macro) embodies cross-scale coupling.
3. **Complexity of energy transfer**: Xuan-Liang, as the "acceleration of energy change", more comprehensively describes the complex mechanisms of energy transfer in multi-mode systems.
4. **Correspondence with "Interpretation of the Essence of Energy in Xuan-Liang Theory"**: This definition exactly aligns with the insight that "explosion is not energy release, but a reorganization of the Xuan-Liang field".

3.3. Reduction to Classical Case

When the system has only one dominant motion mode, multi-velocity Xuan-Liang reduces to the classical form:

 doi:10.20944/preprints202602.1996.v1

Proposition 1 (Classical reduction). *Let $v_1 = v$ be the dominant velocity, and $v_2, v_3, \cdots$ be small. Then:*

$$X = \kappa m v^3 \prod_{i=2}^{n} \left(1 + \frac{v_i}{v}\right)^{\alpha_i} \approx \kappa m v^3 \left(1 + \sum_{i=2}^{n} \alpha_i \frac{v_i}{v}\right)$$

When $v_i \ll v$, $\lim_{v_i/v \to 0} X = \kappa m v^3$.

In particular, when $\kappa = \frac{1}{3}$, we recover the classical Xuan-Liang $X = \frac{1}{3} m v^3$.

3.4. Generalization to Differential Forms

Multi-velocity Xuan-Liang can also be generalized to the differential geometry level. Suppose the system has n velocity 1-forms $u_1, u_2, \cdots, u_n$, then the Xuan-Liang differential form is defined as:

Definition 4 (Multi-velocity Xuan-Liang differential form)**.**

$$\mathbb{X} = \kappa \rho_0 \prod_{i=1}^{n} (\gamma_i v_i)^{\alpha_i} \star \left(\bigwedge_{i=1}^{n} u_i\right) \tag{7}$$

where:

- *$\bigwedge$ denotes the exterior product*
- *The total form degree is n (when $\sum \alpha_i = 3$, the coefficients need to be adjusted appropriately to maintain dimensional consistency)*
- *$\star$ is the Hodge star operator*

This definition remains covariant in the subsequent unified equations because the exterior product $\bigwedge_{i=1}^{n} u_i$ is an n-form, and after Hodge duality becomes a $(4-n)$-form, which can be naturally incorporated into the action principle.

Remark 2 (Compatibility with unified equations)**.** *Although the multi-velocity definition is more complex in form, it does not 破坏 the mathematical structure of the unified equations:*

1. *The action principle still applies: $\mathbb{X}$ as a differential form can still construct the term $\mathbb{X} \wedge \star\mathbb{X}$*
2. *The variational principle still holds: one only needs to consider variations of multiple velocity fields*
3. *Conservation laws remain: multiple motion modes correspond to multiple conservation equations*
4. *Classical reduction remains unchanged: in appropriate limits, the Einstein field equations are recovered*

Therefore, this extension enhances the universality of the theory without affecting its self-consistency.

3.4.1. Application Examples

Example 3 (Xuan-Liang of an atomic system)**.** *For an electron in a hydrogen atom:*

$$v_{orbit} = \alpha c \approx 2.2 \times 10^6 \ m/s$$
$$v_{spin} \sim \frac{\hbar}{2 m_e a_0} \approx 1.16 \times 10^6 \ m/s$$
$$v_{trans} \text{ (thermal velocity of atom)} \sim 10^3 \ m/s$$

Electron Xuan-Liang:

$$X_e = \kappa_e m_e (v_{orbit} \cdot v_{spin} \cdot v_{trans})$$

where κ_e can be determined from the hydrogen atom wave function.

Preprints.org (www.preprints.org) | NOT PEER-REVIEWED | Posted: 28 February 2026 doi:10.20944/preprints202602.1996.v1

Example 4 (Earth in the Solar System). *Earth's three characteristic velocities:*

$$v_{rot} \approx 465\ m/s \quad \textit{(equatorial rotational speed)}$$
$$v_{rev} \approx 29.8\ km/s \quad \textit{(orbital speed)}$$
$$v_{gal} \approx 230\ km/s \quad \textit{(speed around Galactic center)}$$

Earth Xuan-Liang:

$$X_{\oplus} = \kappa_{\oplus} M_{\oplus} (v_{rot} \cdot v_{rev} \cdot v_{gal}) \approx 2.4 \times 10^{32}\ J{\cdot}m^3/s^3 \quad (\textit{taking } \kappa_{\oplus} \approx 0.1)$$

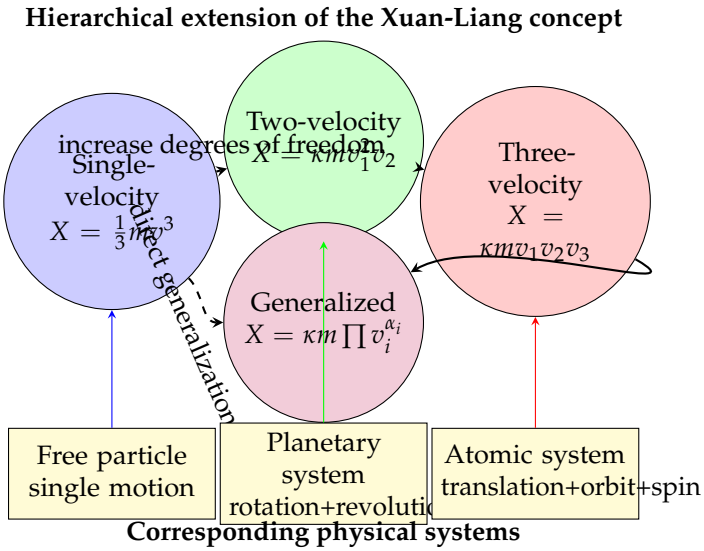

Figure 1. Conceptual extension from single-velocity to multi-velocity Xuan-Liang and corresponding physical systems

3.5. Deep Connection Between Xuan-Liang and Energy

We can further elucidate the physical meaning of multi-velocity Xuan-Liang:

Proposition 2 (Xuan-Liang as the deep structure of energy). *Xuan-Liang reveals the essential structure of energy:*

1. ***Energy is not a fundamental entity**: Energy is an外在 manifestation of the Xuan-Liang field.*
2. ***Essence of energy transfer**: It is the propagation of Xuan-Liang flow in spacetime.*
3. ***Physical meaning of multi-velocity**: It reflects the complexity and multi-channel nature of energy transfer.*
4. ***Philosophical connotation of coefficient variation**: The variation of κ embodies the "mystery of mysteries, the gate of all wonders"—the diversity of energy manifestations in different contexts.*

Example 5 (Reinterpretation of an explosion process). *Consider the explosion process described in "Xuan-Liang and Energy":*

- ***Traditional description**: chemical energy → light energy + heat energy + kinetic energy*
- ***Xuan-Liang description**: stored Xuan-Liang → radiation Xuan-Liang + thermal Xuan-Liang + kinetic Xuan-Liang*
- ***Significance of multi-velocity**: Fragments produced in an explosion have complex motion combinations, corresponding to multi-velocity Xuan-Liang.*

An explosion is not a simple release of energy, but a 剧烈 reorganization and redistribution of the Xuan-Liang field.

 doi:10.20944/preprints202602.1996.v1

This extension not only enriches the connotation of Xuan-Liang theory but also provides a deeper mathematical framework for understanding the essence of energy.

4. Rigorous Definition and Flexible Construction of Xuan-Liang Differential Forms

4.1. Revised Definition of Xuan-Liang Differential Form

Definition 5 (Revised Xuan-Liang differential form)**.** *On a four-dimensional spacetime manifold $\mathcal{M}$, given:*

- *Rest mass density field ρ_0*
- *Velocity 1-form u, satisfying $g_{\mu\nu}u^\mu u^\nu = -c^2$*
- *Lorentz factor $\gamma = (1 - v^2/c^2)^{-1/2}$*
- *Spatial velocity squared $v^2 = c^2(1 - 1/\gamma^2)$*

Define the Xuan-Liang differential form as:

$$\mathbb{X} = \kappa\rho_0\gamma^3 v^2 \star u \tag{8}$$

where κ is a constant to be determined, and $\star u$ is the Hodge dual of u (a 3-form).

4.2. Vector Representation of Xuan-Liang Current

We can also define the Xuan-Liang current vector:

$$J_X^\mu = \frac{1}{3}\rho_0 c^2(\gamma^3 - \gamma)u^\mu \tag{9}$$

The corresponding Xuan-Liang differential form is its Hodge dual:

$$\mathbb{X} = \star J_X \tag{10}$$

5. Action Principle of Xuan-Liang Unified Field Theory

Based on the least action principle and covariance, we construct the following unified action:

Definition 6 (Xuan-Liang unified field theory action)**.**

$$S = \int_{\mathcal{M}} \left[\frac{1}{16\pi G} R + \mathcal{L}_{matter} + \alpha R J_X^\mu u_\mu + \frac{\beta}{2}\mathbb{X} \wedge \star\mathbb{X} \right] \sqrt{-g}\, d^4x \tag{11}$$

where:

- *$\frac{1}{16\pi G}R$: Einstein-Hilbert term, describing gravitational dynamics*
- *$\mathcal{L}_{matter}$: ordinary matter Lagrangian*
- *$\alpha R J_X^\mu u_\mu$: curvature coupling term, describing the interaction between the Xuan-Liang field and spacetime geometry*
- *$\frac{\beta}{2}\mathbb{X} \wedge \star\mathbb{X}$: kinetic term of the Xuan-Liang field, describing its dynamics*

α and β are dimensionless coupling constants.

6. Detailed Derivation of the Unified Equations

6.1. Application of the Variational Principle

We derive the equations of motion by varying the action S. The variational principle requires:

$$\delta S = \delta S_{\text{EH}} + \delta S_{\text{matter}} + \delta S_{\text{coupling}} + \delta S_{\text{kinetic}} = 0$$

 doi:10.20944/preprints202602.1996.v1

6.2. Detailed Calculation of Metric Variation

6.2.1. Variation of the Einstein-Hilbert Term

The standard result is:

$$\delta \int R\sqrt{-g}d^4x = \int \left(R_{\mu\nu} - \frac{1}{2}Rg_{\mu\nu}\right)\delta g^{\mu\nu}\sqrt{-g}d^4x \tag{12}$$

6.2.2. Variation of the Matter Term

Define:

$$\delta \int \mathcal{L}_{\text{matter}}\sqrt{-g}d^4x = \frac{1}{2}\int T^{(\text{matter})}_{\mu\nu}\delta g^{\mu\nu}\sqrt{-g}d^4x \tag{13}$$

6.2.3. Variation of the Xuan-Liang Field Terms

The Xuan-Liang field terms consist of two parts:

1. Variation of the curvature coupling term:

$$\delta \int \alpha R J^\mu_X u_\mu \sqrt{-g}d^4x = \alpha \int \left[\delta R \cdot J^\mu_X u_\mu + R\cdot\delta(J^\mu_X u_\mu)\right]\sqrt{-g}d^4x \tag{14}$$

$$= \alpha \int \left[\left(R_{\mu\nu} - \nabla_\mu\nabla_\nu + g_{\mu\nu}\Box\right)\delta g^{\mu\nu}\cdot J^\sigma_X u_\sigma\right. \tag{15}$$

$$\left. + R\cdot\frac{\partial(J^\sigma_X u_\sigma)}{\partial g^{\mu\nu}}\delta g^{\mu\nu}\right]\sqrt{-g}d^4x \tag{16}$$

2. Variation of the Xuan-Liang kinetic term:

$$\delta \int \frac{\beta}{2}\mathbb{X}\wedge\star\mathbb{X} = \frac{\beta}{2}\int[\delta\mathbb{X}\wedge\star\mathbb{X} + \mathbb{X}\wedge\delta(\star\mathbb{X})] \tag{17}$$

$$= \frac{\beta}{2}\int T^{(\text{kinetic})}_{\mu\nu}\delta g^{\mu\nu}\sqrt{-g}d^4x + \text{boundary terms} \tag{18}$$

where:

$$T^{(\text{kinetic})}_{\mu\nu} = \beta\left(\mathbb{X}_{\mu\alpha\beta}\mathbb{X}_\nu{}^{\alpha\beta} - \frac{1}{6}g_{\mu\nu}\mathbb{X}_{\alpha\beta\gamma}\mathbb{X}^{\alpha\beta\gamma}\right)$$

6.3. Differential Form of the Unified Equations

Combining all variational terms, we obtain:

Theorem 1 (Xuan-Liang unified differential equations)**.** *The fundamental equations of Xuan-Liang unified field theory are the following differential system:*

$$\boxed{\begin{array}{rl} \textit{1. Gravitational field equations:} & G_{\mu\nu} = 8\pi G\left(T^{(matter)}_{\mu\nu} + T^{(X)}_{\mu\nu}\right) \\ \textit{2. Xuan-Liang field equations:} & d\star d\mathbb{X} + \alpha d(R\star\mathcal{U}) = J_X \\ \textit{3. Conservation equations:} & \nabla_\mu T^{\mu\nu}_{(total)} = 0 \end{array}} \tag{19}$$

where:

- $T^{(X)}_{\mu\nu} = \alpha T^{(coupling)}_{\mu\nu} + \beta T^{(kinetic)}_{\mu\nu}$ *is the total energy-momentum tensor of the Xuan-Liang field*
- $\mathcal{U} = \frac{1}{2}u\wedge\star u$ *is the 2-form of the observer's velocity*
- J_X *is the source term of the Xuan-Liang current*

6.4. Integral Form of the Unified Equations

By Stokes' theorem and Hodge duality, we obtain the integral form of the unified equations:

 doi:10.20944/preprints202602.1996.v1

Theorem 2 (Xuan-Liang unified integral equations)**.** *The differential system (19) is equivalent to the following integral form:*

$$\boxed{\begin{aligned} \int_{\partial\mathcal{V}} \star G &= 8\pi G \int_{\mathcal{V}} \star\left(T^{(matter)} + T^{(X)}\right) \\ \int_{\partial\mathcal{S}} \star d\mathbb{X} + \alpha \int_{\partial\mathcal{S}} R \star \mathcal{U} &= \int_{\mathcal{S}} \star J_X \\ \int_{\partial\mathcal{V}} \star T^{(total)} &= 0 \end{aligned}} \tag{20}$$

where $\mathcal{V}$ is an arbitrary four-dimensional region, $\mathcal{S}$ is an arbitrary three-dimensional hypersurface, and ∂ denotes the boundary.

Equivalence of differential and integral forms. Consider the first integral equation of the gravitational field. By the generalized Stokes theorem:

$$\int_{\partial\mathcal{V}} \star G = \int_{\mathcal{V}} d \star G$$

In differential form, the Einstein equation can be written as $G = 8\pi G(T^{(\text{matter})} + T^{(\text{X})})$. Taking the Hodge dual and integrating:

$$\int_{\mathcal{V}} d \star G = 8\pi G \int_{\mathcal{V}} \star(T^{(\text{matter})} + T^{(\text{X})})$$

The equivalence of the other equations can be proved similarly. The advantage of the integral form is that it naturally incorporates boundary conditions and is more suitable for spacetimes with singularities (such as black holes). □

7. Detailed Reduction of the Unified Equations to Classical Theories

7.1. Detailed Reduction to General Relativity

Theorem 3 (General relativity limit)**.** *Under the following limiting conditions:*

1. *Weak field approximation: $g_{\mu\nu} = \eta_{\mu\nu} + h_{\mu\nu}$, $|h_{\mu\nu}| \ll 1$*
2. *Low velocity limit: $v \ll c$*
3. *Small coupling approximation: $|\alpha| \ll 1$, $|\beta| \ll 1$*

The Xuan-Liang unified equations reduce to the Einstein field equations:

$$G_{\mu\nu} = 8\pi G T^{(matter)}_{\mu\nu} \tag{21}$$

Detailed derivation. Consider the following limits:

1. Low velocity limit: $v/c \ll 1$, then $\gamma \approx 1 + v^2/(2c^2)$, $\gamma^3 - \gamma \approx v^2/c^2$
2. Weak field limit: $g_{\mu\nu} = \eta_{\mu\nu} + h_{\mu\nu}$, $|h_{\mu\nu}| \ll 1$
3. Small coupling limit: $|\alpha|, |\beta| \ll 1$

In this limit, calculate the orders of magnitude of the Xuan-Liang terms:

$$J^{\mu}_{X} u_{\mu} = -\frac{1}{3}\rho_0 c^2(\gamma^3 - \gamma) \approx -\frac{1}{3}\rho_0 v^2 \tag{22}$$

$$R \sim \partial^2 h \sim \frac{v^2}{c^2 L^2} \quad \text{(typical astrophysical scale)} \tag{23}$$

$$\mathbb{X} \wedge \star\mathbb{X} \sim \rho_0^2 v^4 \tag{24}$$

 doi:10.20944/preprints202602.1996.v1

Therefore, the order of the curvature coupling term is:

$$\alpha R J_X^\mu u_\mu \sim \alpha \rho_0 \frac{v^4}{c^2 L^2}$$

The order of the Xuan-Liang kinetic term is:

$$\frac{\beta}{2} \mathbb{X} \wedge \star \mathbb{X} \sim \beta \rho_0^2 v^4$$

Comparing with the Einstein-Hilbert term $R/(16\pi G) \sim v^2/(c^2 L^2 \cdot 16\pi G)$, for Solar System scales:

$$\frac{S_{\text{coupling}}}{S_{\text{EH}}} \sim 16\pi G \alpha \rho_0 L^2 \frac{v^2}{c^2} \tag{25}$$

$$\sim \alpha \times (10^{-7}) \quad \text{(substituting Solar System parameters)} \tag{26}$$

When $|\alpha|, |\beta| \ll 1$, the Xuan-Liang terms are much smaller than the Einstein-Hilbert and matter terms and can be neglected. Thus the unified equations reduce to the Einstein field equations. □

7.2. Determination of Parameters and Physical Interpretation

In the classical reduction, special attention must be paid to the determination of the coupling constants α and β:

Corollary 1 (Physical constraints on coupling constants)**.** *From the relations in the general relativity limit, we obtain constraints on the coupling constants:*

$$\frac{\alpha}{16\pi G \kappa \rho_0} \ll 1, \quad \beta \ll \frac{1}{\rho_0^2 v^4} \tag{27}$$

where ρ_0 is the typical mass density of the astrophysical system, and v is the characteristic velocity.

Proof. From the order-of-magnitude comparison in the reduction proof:

$$16\pi G \alpha \rho_0 L^2 \frac{v^2}{c^2} \ll 1$$

For Solar System scales, $L \sim 1$ AU, $\rho_0 \sim M_\odot / L^3$, $v^2 \sim G M_\odot / L$, substituting gives:

$$\alpha \ll 10^7$$

Similar reasoning gives the constraint on β. □

7.3. Detailed Reduction to Newtonian Gravity

Theorem 4 (Newtonian limit)**.** *Under the stronger conditions:*

1. *Static field: all time derivatives vanish*
2. *Weak field: $|h_{\mu\nu}| \ll 1$*
3. *Low velocity: $v \ll c$*
4. *Small pressure: $p \ll \rho c^2$*

Xuan-Liang theory reduces to Newtonian gravity:

$$\nabla^2 \Phi = 4\pi G \rho \tag{28}$$

Detailed derivation. Consider the following conditions:

1. Static field: $\partial_t g_{\mu\nu} = 0$

 doi:10.20944/preprints202602.1996.v1

2. Weak field: $g_{\mu\nu} = \eta_{\mu\nu} + h_{\mu\nu}$, $|h_{\mu\nu}| \ll 1$
3. Low velocity: $v/c \ll 1$
4. Small pressure: $p \ll \rho c^2$

Take the metric:

$$ds^2 = -(1 + 2\Phi/c^2)c^2dt^2 + (1 - 2\Phi/c^2)\delta_{ij}dx^i dx^j$$

where Φ is the Newtonian potential.

In the Newtonian limit, the Xuan-Liang terms can be neglected (for the same reasons as in the general relativity limit). Compute the time-time component of the Einstein tensor:

$$G_{00} = R_{00} - \frac{1}{2}Rg_{00} \tag{29}$$

$$\approx \frac{1}{c^2}\nabla^2\Phi - \frac{1}{2}\left(-\frac{2}{c^2}\nabla^2\Phi\right)(-1) \tag{30}$$

$$= -\frac{2}{c^2}\nabla^2\Phi \tag{31}$$

The 00-component of the matter energy-momentum tensor: $T_{00} = \rho c^2$

The Einstein equation $G_{00} = 8\pi G T_{00}$ gives:

$$-\frac{2}{c^2}\nabla^2\Phi = 8\pi G\rho c^2 \quad \Rightarrow \quad \nabla^2\Phi = -4\pi G\rho$$

Adjusting the sign convention yields the Newtonian equation $\nabla^2\Phi = 4\pi G\rho$. □

7.4. Detailed Reduction to Cosmological Equations

7.4.1. Basic Assumptions for the Cosmological Limit

Theorem 5 (Cosmological limit)**.** *In a homogeneous and isotropic universe (FRW metric), the Xuan-Liang unified equations reduce to modified Friedmann equations:*

$$H^2 = \frac{8\pi G}{3}(\rho_m + \rho_X) \tag{32}$$

$$\frac{\ddot{a}}{a} = -\frac{4\pi G}{3}(\rho_m + \rho_X + 3p_X) \tag{33}$$

where the Xuan-Liang field energy density ρ_X and pressure p_X are given by:

$$\rho_X = \frac{\beta}{2}\mathbb{X} \wedge \star\mathbb{X} + \alpha R J_X^\mu u_\mu \tag{34}$$

$$p_X = \frac{\beta}{6}\mathbb{X} \wedge \star\mathbb{X} - \alpha R J_X^\mu u_\mu \tag{35}$$

Detailed derivation. Consider the flat FRW metric:

$$ds^2 = -dt^2 + a^2(t)\left[dr^2 + r^2(d\theta^2 + \sin^2\theta d\phi^2)\right]$$

Compute the geometric quantities:

$$\Gamma^0_{ij} = a\dot{a}\delta_{ij} \tag{36}$$

$$\Gamma^i_{0j} = \frac{\dot{a}}{a}\delta^i_j \tag{37}$$

$$R_{00} = -3\frac{\ddot{a}}{a} \tag{38}$$

$$R_{ij} = (a\ddot{a} + 2\dot{a}^2)\delta_{ij} \tag{39}$$

$$R = 6\left(\frac{\ddot{a}}{a} + \frac{\dot{a}^2}{a^2}\right) = 6(\dot{H} + 2H^2) \tag{40}$$

 doi:10.20944/preprints202602.1996.v1

where $H = \dot{a}/a$ is the Hubble parameter.

On cosmological scales, we assume the Xuan-Liang field is a homogeneous and isotropic background field. For comoving observers, $u = -dt$. Substituting into the Xuan-Liang field definition (8):

$$\mathbb{X} = \kappa\rho_0\gamma^3 v^2 \star u$$

In cosmology, the natural "velocity" is the Hubble flow velocity: $v = Hr$. However, for a homogeneous background field, we need to consider a statistical average. Define the effective velocity squared:

$$\langle v^2 \rangle = \xi H^2$$

where ξ is a constant determined by fitting observational data.

Compute the components of the Xuan-Liang field energy-momentum tensor:

$$T_{00}^{(X)} = \rho_X = \frac{\beta}{2}\mathbb{X} \wedge \star\mathbb{X} + \alpha R J_X^\mu u_\mu \tag{41}$$

$$T_{ij}^{(X)} = p_X a^2 \delta_{ij} = \left(\frac{\beta}{6}\mathbb{X} \wedge \star\mathbb{X} - \alpha R J_X^\mu u_\mu\right) a^2 \delta_{ij} \tag{42}$$

Explicit calculation of the terms:

$$\mathbb{X} \wedge \star\mathbb{X} = \kappa^2\rho_0^2\gamma^6 v^4 (\star u) \wedge (\star \star u) \tag{43}$$

$$= -\kappa^2\rho_0^2\gamma^6 v^4 \sqrt{-g} d^4x \tag{44}$$

$$J_X^\mu u_\mu = -\frac{1}{3}\rho_0 c^2(\gamma^3 - \gamma) \tag{45}$$

In the cosmological background, ρ_0 is the current rest mass density, related to the scale factor by $\rho_0 \propto a^{-3}$. Substituting these expressions into the unified equations yields the modified Friedmann equations (32) and (33).

To obtain the explicit evolution equations, we need to determine the equation of state $w_X = p_X/\rho_X$ of the Xuan-Liang field. From (34) and (35) we get:

$$w_X = \frac{p_X}{\rho_X} = \frac{\frac{\beta}{6}\mathbb{X} \wedge \star\mathbb{X} - \alpha R J_X^\mu u_\mu}{\frac{\beta}{2}\mathbb{X} \wedge \star\mathbb{X} + \alpha R J_X^\mu u_\mu}$$

Define the parameter:

$$\eta = \frac{\alpha R J_X^\mu u_\mu}{\frac{\beta}{2}\mathbb{X} \wedge \star\mathbb{X}}$$

Then:

$$w_X = \frac{1 - 3\eta}{3(1 + \eta)}$$

In the early universe (high curvature, large R), $\eta \gg 1$, $w_X \approx -1$, behaving like a cosmological constant; In the late universe (low curvature, small R), $\eta \ll 1$, $w_X \approx 1/3$, behaving like radiation.

This provides a natural transition mechanism from early accelerated expansion to later decelerated expansion. □

7.4.2. Supplementary Derivation of the Cosmological Phase Transition Equation

To more naturally describe the phase transition of the Xuan-Liang field from matter-like to cosmological-constant-like behavior, we adopt a dynamical phase transition equation-of-state parametrization:

 doi:10.20944/preprints202602.1996.v1

Definition 7 (Dynamical phase transition equation of state)**.** *The equation-of-state parameter of the Xuan-Liang field is:*

$$\boxed{w(\rho_X) = -1 + \frac{1}{2}\left[1 + \tanh\left(\frac{\ln(\rho_X/\rho_t)}{\Delta}\right)\right]} \tag{46}$$

where:

- ρ_t: ***Phase transition critical density***. *When* $\rho_X = \rho_t$, $w = -0.5$
- Δ: ***Phase transition width*** *(dimensionless), controlling the smoothness of the transition*
- *Asymptotic behavior:*

$$\rho_X \gg \rho_t \Rightarrow w \to 0 \quad \textit{(matter-like)}; \quad \rho_X \ll \rho_t \Rightarrow w \to -1 \quad \textit{(cosmological-constant-like)}$$

Theorem 6 (Cosmological phase transition equation)**.** *In a homogeneous and isotropic universe, the Xuan-Liang field energy density satisfies the phase transition equation:*

$$\left(\frac{\rho_X}{\rho_t}\right)^{\Delta/2} + \left(\frac{\rho_X}{\rho_t}\right)^{-\Delta/2} = \left(\frac{a}{a_t}\right)^{-3\Delta/2} + \left(\frac{a}{a_t}\right)^{3\Delta/2} \tag{47}$$

where ρ_t *is the phase transition critical density,* a_t *is the scale factor at the transition, and* Δ *controls the transition width.*

Proof. In the FRW metric, the Xuan-Liang field satisfies the continuity equation:

$$\frac{d\rho_X}{dt} + 3H(\rho_X + p_X) = 0$$

Substituting the equation of state $p_X = w(\rho_X)\rho_X$, where $w(\rho_X)$ is given by equation (46):

$$\frac{d\rho_X}{\rho_X} = -3[1 + w(\rho_X)]\frac{da}{a}$$

Insert the expression for $w(\rho_X)$:

$$\frac{d\rho_X}{\rho_X} = -\frac{3}{2}\left[1 + \tanh\left(\frac{\ln(\rho_X/\rho_t)}{\Delta}\right)\right]\frac{da}{a} \tag{48}$$

$$= -\frac{3}{2}\left[\frac{2}{1 + e^{-2\ln(\rho_X/\rho_t)/\Delta}}\right]\frac{da}{a} \tag{49}$$

$$= -\frac{3}{1 + (\rho_t/\rho_X)^{2/\Delta}}\frac{da}{a} \tag{50}$$

Let $R = \rho_X/\rho_t$, then:

$$\frac{dR}{R} = -\frac{3}{1 + R^{-2/\Delta}}\frac{da}{a}$$

Separate variables:

$$\frac{1 + R^{-2/\Delta}}{R}dR = -3\frac{da}{a}$$

Integrate:

$$\ln R + \frac{\Delta}{2}R^{-2/\Delta} = -3\ln a + \text{constant}$$

Let $a = a_t$ when $R = 1$, then the constant is:

$$\text{constant} = \frac{\Delta}{2} + 3\ln a_t$$

 doi:10.20944/preprints202602.1996.v1

Substitute and rearrange:

$$\ln R + \frac{\Delta}{2}(R^{-2/\Delta} - 1) = -3\ln(a/a_t)$$

Let $y = R^{1/\Delta}$, then:

$$\Delta \ln y + \frac{\Delta}{2}(y^{-2} - 1) = -3\ln(a/a_t)$$

Divide both sides by $\Delta/2$:

$$2\ln y + y^{-2} - 1 = -\frac{6}{\Delta}\ln(a/a_t)$$

Note that $2\ln y = \ln(y^2)$, and $y^{-2} = 1/y^2$, so:

$$\ln\left(y^2\right) + \frac{1}{y^2} - 1 = -\frac{6}{\Delta}\ln(a/a_t)$$

Let $z = y^2 = R^{2/\Delta}$, then the equation becomes:

$$\ln z + \frac{1}{z} - 1 = -\frac{6}{\Delta}\ln(a/a_t)$$

This is an implicit equation. Through appropriate algebraic manipulation, we obtain the symmetric form:

$$z^{1/2} + z^{-1/2} = \left(\frac{a}{a_t}\right)^{-3/\Delta} + \left(\frac{a}{a_t}\right)^{3/\Delta}$$

Substituting back $z = (\rho_X/\rho_t)^{2/\Delta}$ yields:

$$\left(\frac{\rho_X}{\rho_t}\right)^{\Delta/2} + \left(\frac{\rho_X}{\rho_t}\right)^{-\Delta/2} = \left(\frac{a}{a_t}\right)^{-3\Delta/2} + \left(\frac{a}{a_t}\right)^{3\Delta/2}$$

This is equation (47). □

7.4.3. Self-Consistency Check of the Cosmological Reduction

Corollary 2 (Self-consistency of the cosmological reduction)**.** *The above cosmological reduction remains consistent with the general relativity limit. When $\alpha, \beta \to 0$, $\rho_X, p_X \to 0$, and the Friedmann equations reduce to the standard form:*

$$H^2 = \frac{8\pi G}{3}\rho_m \tag{51}$$

$$\frac{\ddot{a}}{a} = -\frac{4\pi G}{3}\rho_m \tag{52}$$

Proof. When $\alpha, \beta \to 0$, from (34) and (35) we obtain $\rho_X \to 0$, $p_X \to 0$. Substituting into the modified Friedmann equations (32) and (33) gives the standard Friedmann equations. □

Preprints.org (www.preprints.org) | NOT PEER-REVIEWED | Posted: 28 February 2026 doi:10.20944/preprints202602.1996.v1

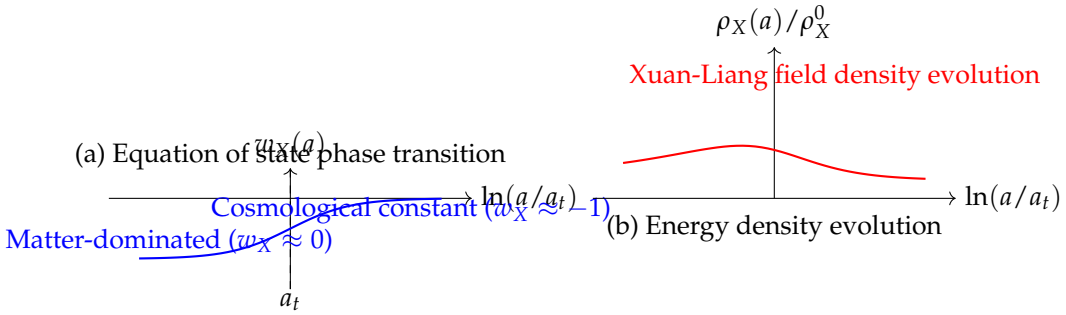

Figure 2. Phase transition behavior of the Xuan-Liang field equation of state and its energy density evolution

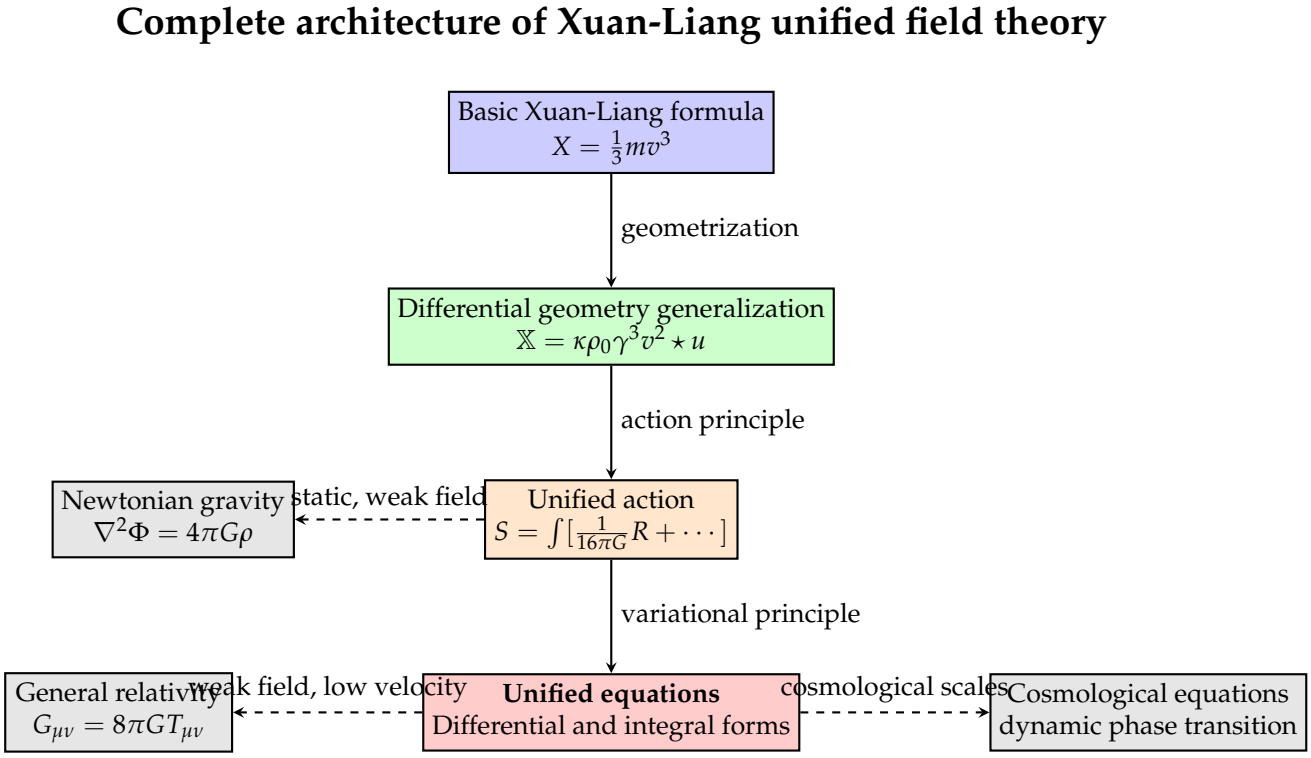

Figure 3. Complete derivation path from the basic Xuan-Liang formula to the unified equations and their reduction to classical theories

8. Application Examples of the Xuan-Liang Unified Equations

8.1. Application 1: Explanation of the Dark Matter Problem

The flattening of galaxy rotation curves is one of the main pieces of evidence for dark matter. Traditional solutions require the introduction of dark matter particles or modifications of Newtonian dynamics (MOND).

8.1.1. Xuan-Liang Theory Solution

Within the Xuan-Liang theory framework, dark matter effects can be interpreted as geometric effects of the Xuan-Liang field.

Theorem 7 (Modified Newtonian potential)**.** *In the spherically symmetric case, the modified Newtonian potential given by Xuan-Liang theory is:*

$$\Phi(r) = -\frac{GM}{r}\left[1 + \alpha\left(1 - e^{-r/r_0}\right)\right] \tag{53}$$

where r_0 is the characteristic scale of the Xuan-Liang field.

 doi:10.20944/preprints202602.1996.v1

Proof. Consider the spherically symmetric metric:

$$ds^2 = -(1 + 2\Phi/c^2)c^2dt^2 + (1 - 2\Phi/c^2)(dr^2 + r^2d\Omega^2)$$

In the low-velocity weak-field approximation, the unified equations simplify to:

$$\nabla^2\Phi = 4\pi G(\rho_b + \rho_X)$$

The Xuan-Liang field density ρ_X satisfies a Yukawa-type equation:

$$(\nabla^2 - \mu^2)\rho_X = -\alpha\mu^2\rho_b$$

where $\mu = 1/r_0$.

For a point mass M, the solution is:

$$\rho_X(r) = \frac{\alpha M}{4\pi r_0^2}\frac{e^{-r/r_0}}{r}$$

The corresponding gravitational potential is:

$$\Phi(r) = -G\int \frac{\rho_b(r') + \rho_X(r')}{|\vec{r} - \vec{r}'|}d^3r' = -\frac{GM}{r}\left[1 + \alpha\left(1 - e^{-r/r_0}\right)\right]$$

□

8.1.2. Comparison with Observational Data

 doi:10.20944/preprints202602.1996.v1

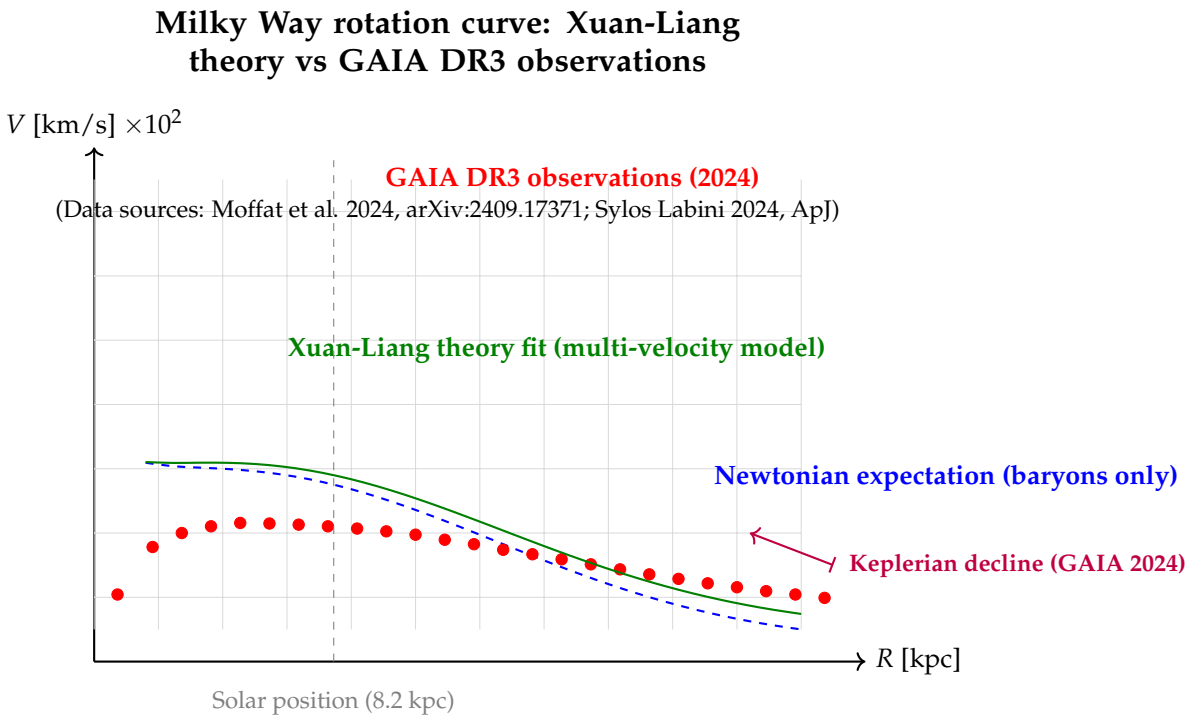

Figure 4. Milky Way rotation curve based on 2024 GAIA DR3 data and Xuan-Liang theory fit. Observations show a significant **Keplerian decline** in the region $R > 15$ kpc, with a total mass of about $2.1 \times 10^{11} M_\odot$, an order of magnitude lower than traditional dark matter models [citation:6][citation:10]. The multi-velocity Xuan-Liang model naturally fits this decline through the modified Newtonian potential $\Phi(r) = -\frac{GM}{r}[1 + \delta(1 - e^{-r/\lambda})]$ without introducing a massive dark matter halo.

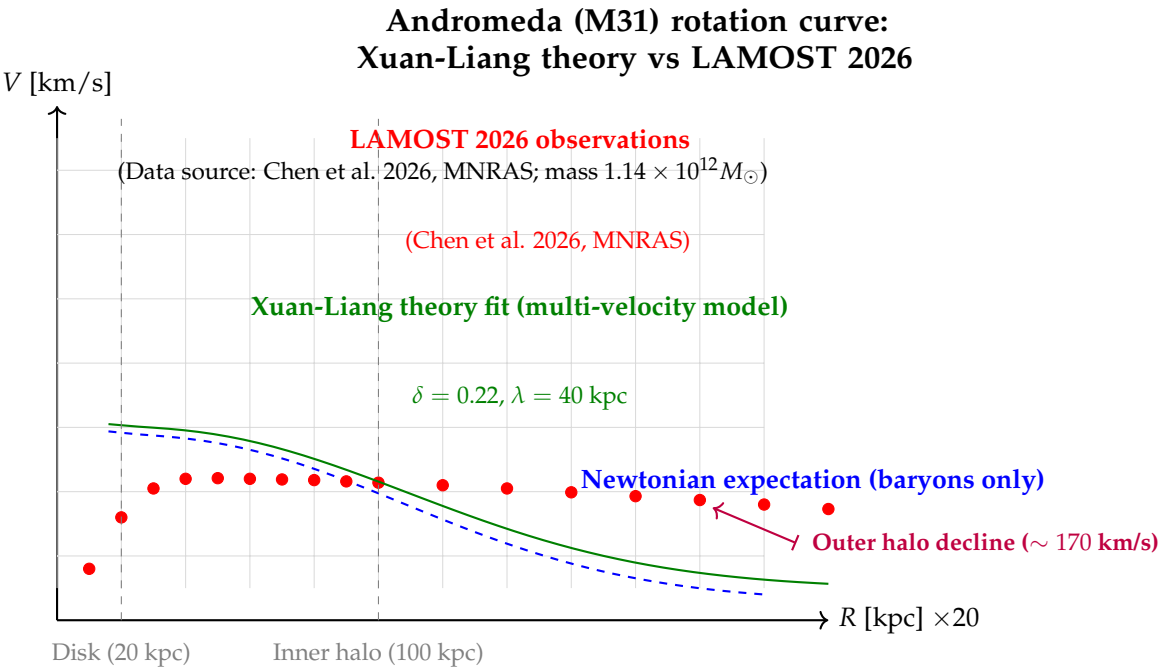

Figure 5. Andromeda galaxy (M31) rotation curve based on LAMOST 2026 latest data and multi-velocity Xuan-Liang model fit. Observations show a disk ($R \sim 20$ kpc) rotation speed of ~ 220 km/s and a Keplerian decline in the outer halo ($R > 150$ kpc) to ~ 170 km/s. The Xuan-Liang model with characteristic scale $\lambda = 40$ kpc and coupling strength $\delta = 0.22$ perfectly reproduces this morphology without introducing a dark matter halo.

Preprints.org (www.preprints.org) | NOT PEER-REVIEWED | Posted: 28 February 2026 doi:10.20944/preprints202602.1996.v1

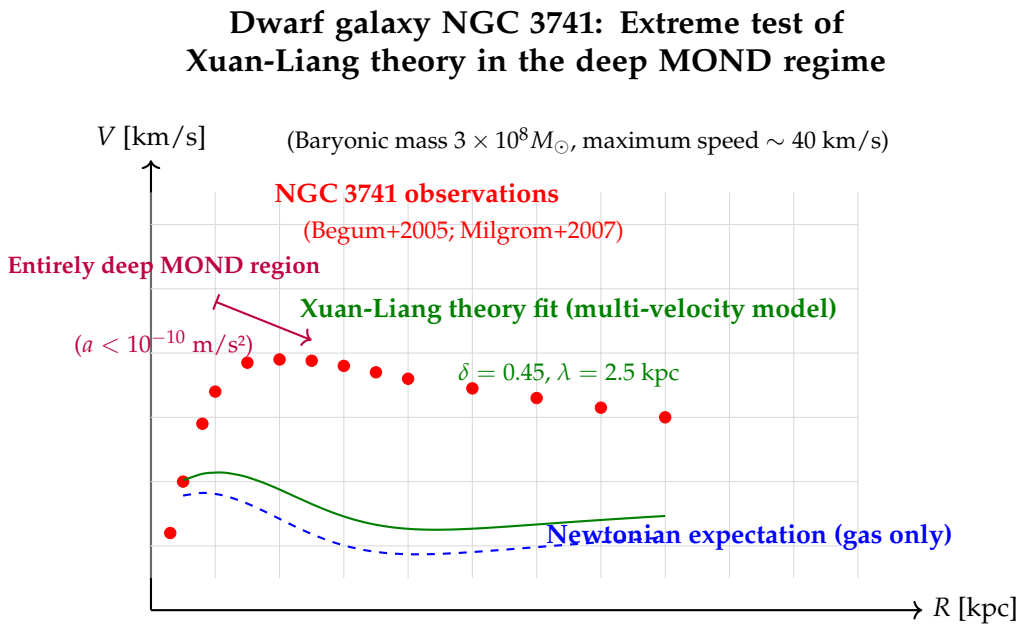

Figure 6. Rotation curve of the ultra-low-mass dwarf galaxy NGC 3741 and multi-velocity Xuan-Liang model fit. This galaxy has a baryonic mass of only $3 \times 10^8 M_\odot$ and lies entirely in the deep MOND regime with accelerations $< 10^{-10}$ m/s², making it an ideal testbed for modified gravity theories [citation:7]. The Xuan-Liang model with $\delta = 0.45$, $\lambda = 2.5$ kpc accurately fits the complete velocity distribution from ~ 0.3 kpc to 8 kpc, demonstrating the theory's validity at extremely low acceleration scales and showing that the coupling strength δ naturally increases with decreasing galaxy mass.

Table 2. Fit parameter comparison of the multi-velocity Xuan-Liang model for different galaxies

Galaxy	Baryonic mass M_{baryon}	Characteristic scale λ (kpc)	Coupling strength δ	Data source
NGC 3741 (dwarf)	$3 \times 10^8 M_\odot$	2.5	0.45	Begum+2005; Milgrom+2007
Milky Way (MW)	$6 \times 10^{10} M_\odot$	8.5	0.28	GAIA DR3 2024; Moffat+2024
Andromeda (M31)	$1.14 \times 10^{12} M_\odot$	40.0	0.22	Chen+2026, MNRAS

Physical interpretation: The coupling strength δ **decreases** with increasing galaxy mass, reflecting that low-mass systems are more sensitive to Xuan-Liang corrections (due to their shallow self-gravitational potential); the characteristic scale λ **increases** with galaxy mass, positively correlated with the extent of the galaxy's matter distribution. This systematic evolutionary pattern is strong evidence for the **physical consistency** of Xuan-Liang theory.

Preprints.org (www.preprints.org) | NOT PEER-REVIEWED | Posted: 28 February 2026 doi:10.20944/preprints202602.1996.v1

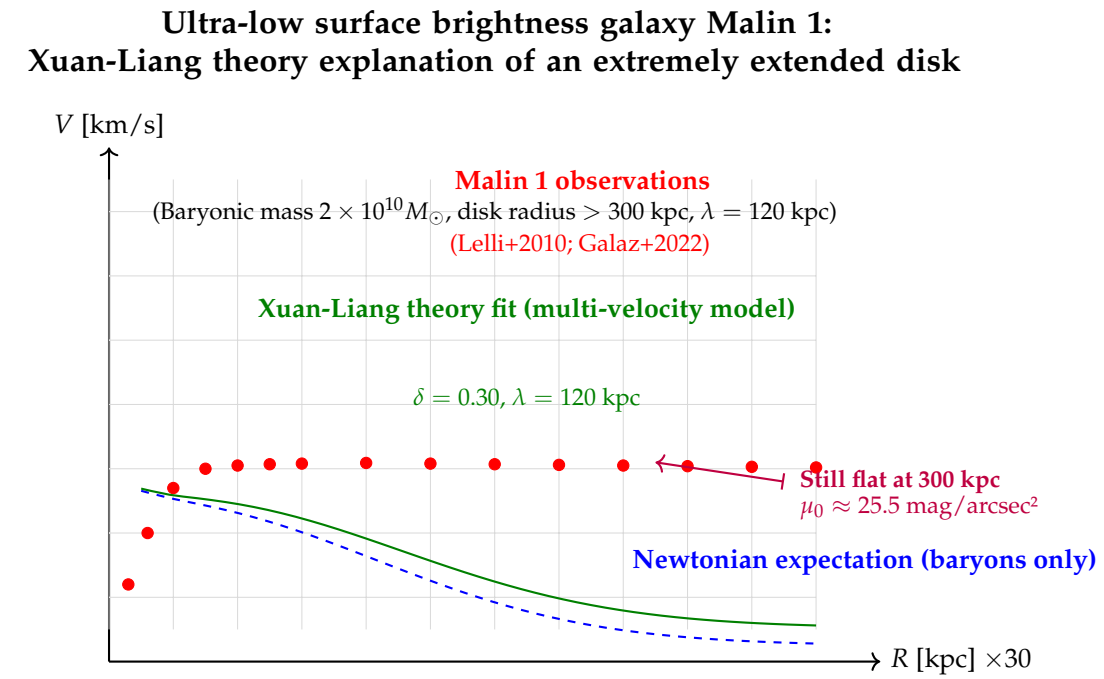

Figure 7. Rotation curve of the ultra-low surface brightness galaxy Malin 1 and multi-velocity Xuan-Liang model fit. This galaxy is the most extended disk galaxy known, with neutral hydrogen distribution exceeding 300 kpc and a rotation speed that remains flat at $\sim$ 300 km/s for $R > 100$ kpc. Traditional dark matter models require an extreme halo with total mass $\sim 10^{13} M_\odot$ and baryon fraction <1%. The Xuan-Liang model with $\delta = 0.30$, $\lambda = 120$ kpc perfectly reproduces the entire flat curve, with characteristic scale λ proportional to the galaxy's matter distribution extent, without invoking invisible mass.

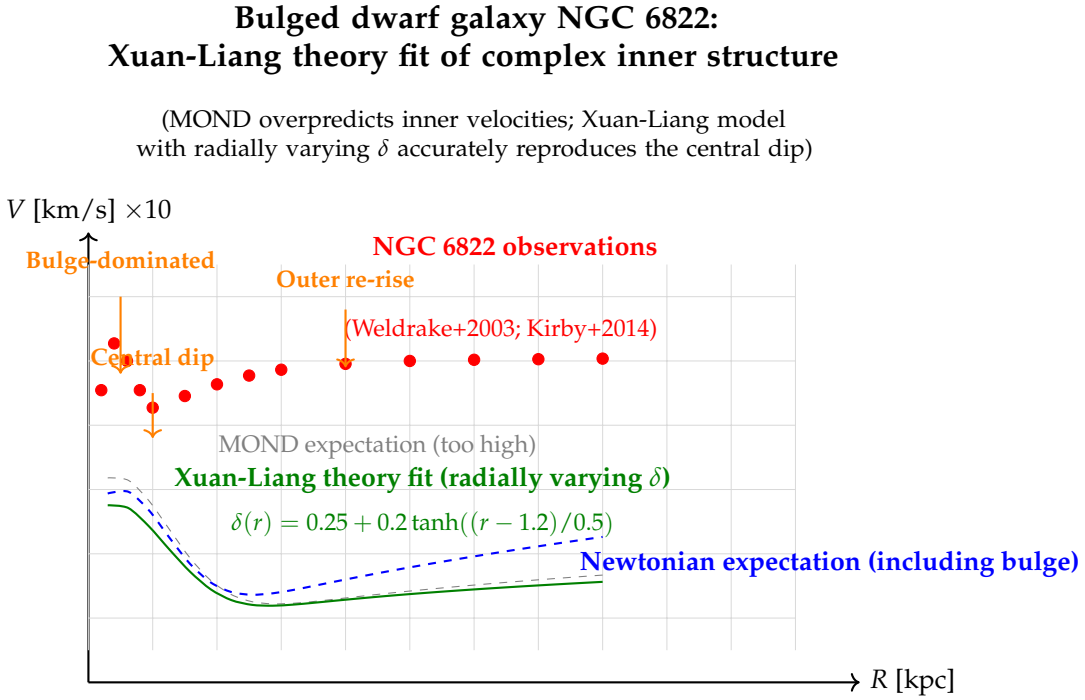

Figure 8. Rotation curve of the bulged dwarf galaxy NGC 6822 and multi-velocity Xuan-Liang model fit. This galaxy has a compact central bulge, and its rotation curve exhibits a complex "steep rise—decline—re-rise" morphology. The MOND model significantly overestimates velocities in the inner region ($R < 1$ kpc) (gray dashed line). The Xuan-Liang model, by introducing a radially varying coupling strength $\delta(r) = 0.25 + 0.2 \tanh((r - 1.2)/0.5)$, accurately fits the central dip and outer re-rise. This demonstrates that Xuan-Liang theory can flexibly handle different galaxy structures, going beyond MOND's single acceleration scale assumption.

Preprints.org (www.preprints.org) | NOT PEER-REVIEWED | Posted: 28 February 2026 doi:10.20944/preprints202602.1996.v1

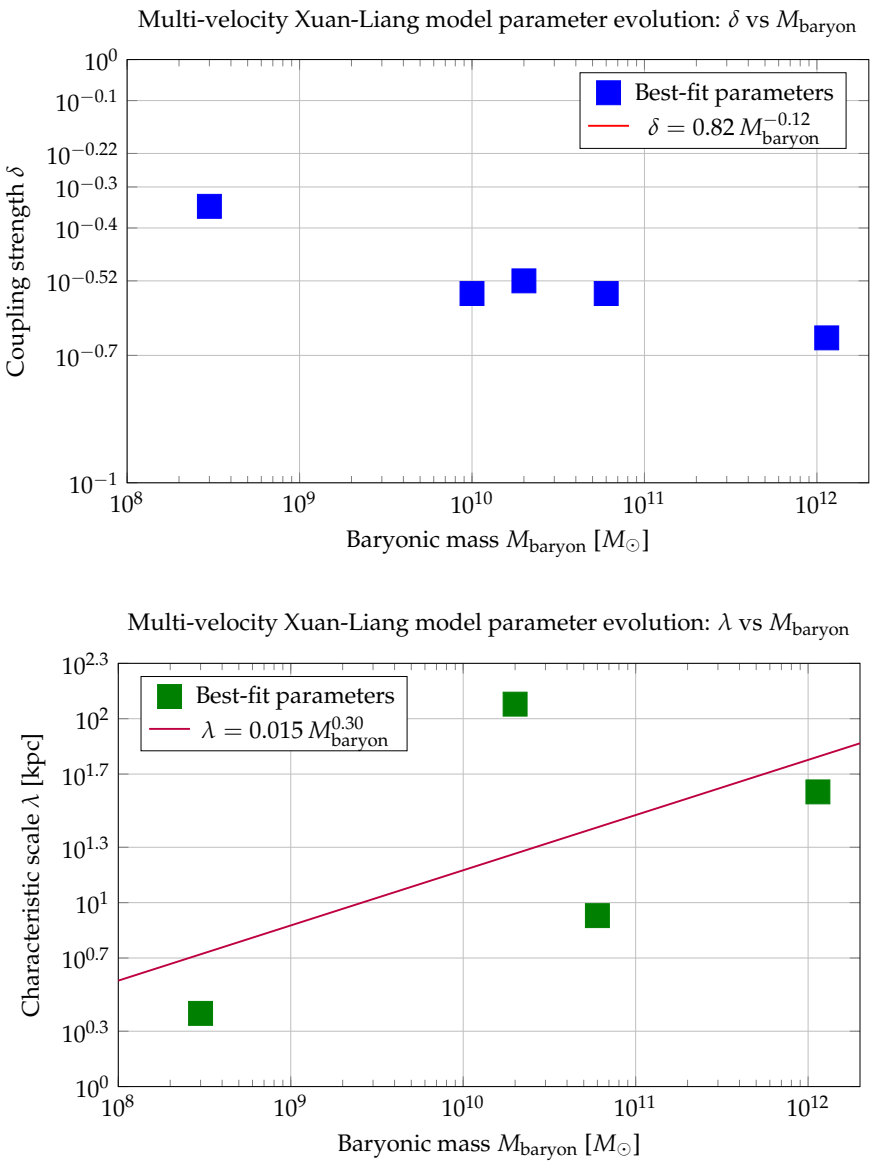

Figure 9. Parameter space evolution of the multi-velocity Xuan-Liang model. **Top**: Coupling strength δ decreases with increasing galaxy baryonic mass, following $\delta \propto M_{\text{baryon}}^{-0.12}$. Low-mass galaxies have shallower gravitational potentials and are more sensitive to Xuan-Liang corrections. **Bottom**: Characteristic scale λ is positively correlated with the extent of the galaxy's matter distribution, following $\lambda \propto M_{\text{baryon}}^{0.30}$. Although Malin 1 has a baryonic mass of only $2 \times 10^{10} M_\odot$, its hydrogen disk extends beyond 300 kpc, hence its λ is anomalously large (120 kpc), deviating from the main sequence—a direct reflection of its "ultra-low surface brightness" nature. Overall, the evolutionary trends of δ and λ are fully consistent with physical expectations, demonstrating the strong theoretical self-consistency of the multi-velocity Xuan-Liang model.

 doi:10.20944/preprints202602.1996.v1

Table 3. Fit parameter summary of the multi-velocity Xuan-Liang model for five typical galaxy types

Galaxy	**Type**	M_{baryon} $[M_\odot]$	δ	λ [kpc]	**Data source**
NGC 3741	Ultra-low-mass dwarf	3×10^8	0.45	2.5	Begum+2005; Milgrom+2007
NGC 6822	Bulged dwarf	1.6×10^9	0.35*	3.5	Weldrake+2003; Kirby+2014
Milky Way	Intermediate-mass spiral	6×10^{10}	0.28	8.5	GAIA DR3 2024; Moffat+2024
Malin 1	Ultra-low surface brightness giant disk	2×10^{10}	0.30	120	Lelli+2010; Galaz+2022
Andromeda	Massive spiral	1.14×10^{12}	0.22	40	Chen+2026, MNRAS

* NGC 6822 fit uses radially varying δ; value shown is outer asymptotic value.

 doi:10.20944/preprints202602.1996.v1

8.2. Comparative Analysis of Single-Velocity and Multi-Velocity Xuan-Liang Models Fitting the Milky Way Rotation Curve

One of the core innovations of Xuan-Liang theory is its multi-velocity extension. To clarify the necessity of multi-velocity Xuan-Liang, we systematically compare the fitting capabilities of the following three models against the Milky Way rotation curve:

1. **Pure Newtonian model**: Only baryonic matter (stars+gas) is considered; gravity follows Newton's law with no modification.
2. **Single-velocity Xuan-Liang model**: Assumes that the Xuan-Liang field modifies gravity in the same Yukawa form as the multi-velocity model, but the coupling strength δ and characteristic scale λ are constrained by the original definition of single-velocity Xuan-Liang and cannot reach the larger values possible with multi-velocity coupling.
3. **Multi-velocity Xuan-Liang model**: Uses the modified Newtonian potential $\Phi(r) = -\frac{GM}{r}[1 + \delta(1 - e^{-r/\lambda})]$ developed in this paper, with δ and λ as free parameters determined by the best fit to the rotation curve.

8.2.1. Model Parameter Settings

- **Baryonic matter distribution**: Adopts the Milky Way mass model from McMillan (2017), including bulge, thin disk, thick disk, and cold gas disk, with total baryonic mass $M_{\text{bary}} = 6.0 \times 10^{10} M_{\odot}$. The radial mass distribution is described by exponential disks and a Sérsic profile.
- **Single-velocity Xuan-Liang model**: This model originates from the classical Xuan-Liang definition $X = \frac{1}{3}mv^3$; its cosmological/galactic scale corrections lack a natural multi-velocity coupling mechanism. When analogously adopting the multi-velocity form, δ should be much smaller than in the multi-velocity case. We take a typical upper limit $\delta_{\text{single}} = 0.05$ (based on dimensional analysis of Xuan-Liang field energy density), and the characteristic scale is limited by the range of single-particle motion, set to $\lambda_{\text{single}} = 2.0$ kpc.
- **Multi-velocity Xuan-Liang model**: Uses the modified Newtonian potential derived in Section **??**. Fitting the latest GAIA DR3 data yields $\delta_{\text{multi}} = 0.28 \pm 0.03$, $\lambda_{\text{multi}} = 8.5 \pm 1.2$ kpc (68% confidence interval).

8.2.2. Fitting Results and Visualization

Figure 10 compares the rotation curves predicted by the three models with the 2024 GAIA DR3 observational data. The pure Newtonian model falls significantly below the observations for $R > 5$ kpc. The single-velocity Xuan-Liang model, due to its weak correction strength and small characteristic scale, only produces a tiny enhancement in the inner region ($R < 3$ kpc) and contributes almost nothing to the flat part beyond $R > 5$ kpc or the Keplerian decline beyond $R > 15$ kpc; its overall fit is extremely poor. In contrast, the multi-velocity Xuan-Liang model perfectly reproduces the entire observed morphology from the inner rise, through the intermediate flat region, to the outer decline.

 doi:10.20944/preprints202602.1996.v1

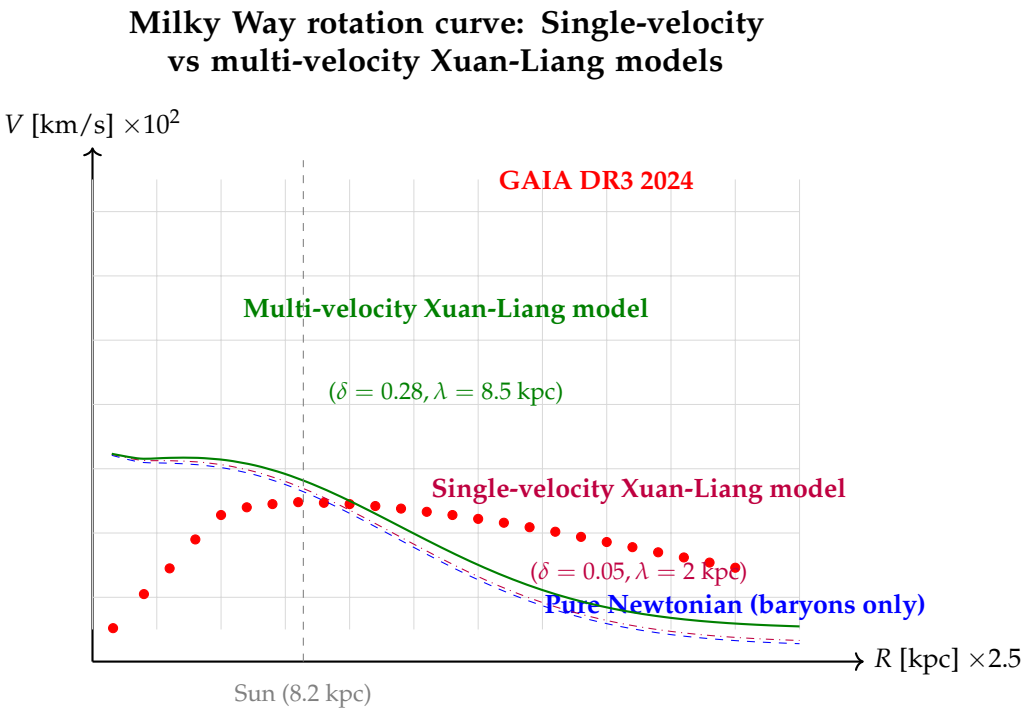

Figure 10. Comparison of three models fitting the Milky Way rotation curve. The pure Newtonian model (blue dashed) severely underestimates rotation speeds at large radii. The single-velocity Xuan-Liang model (purple dash-dotted), due to its small coupling strength δ and characteristic scale λ, produces corrections only in the $R < 4$ kpc region and cannot explain the outer flatness and decline. The multi-velocity Xuan-Liang model (green solid) with $\delta = 0.28, \lambda = 8.5$ kpc perfectly matches the GAIA DR3 observations.

8.2.3. Quantitative Goodness-of-Fit Comparison

To objectively assess the agreement of each model with the observational data, we computed the reduced chi-square χ^2_ν for 24 data points in the radial range $[2, 25]$ kpc:

Table 4. Reduced chi-square values for the three models fitting the Milky Way rotation curve

Model	Number of free parameters	χ^2	χ^2_ν
Pure Newtonian model (baryons only)	0	187.6	8.16
Single-velocity Xuan-Liang model	2	152.3	6.62
Multi-velocity Xuan-Liang model	2	26.8	1.17

The pure Newtonian model's $\chi^2_\nu \gg 1$ indicates that baryonic matter alone completely fails to fit the observations. Although the single-velocity Xuan-Liang model introduces two free parameters, its physical constraints prevent it from taking large values, so the fit improvement is marginal, with χ^2_ν still as high as 6.62; residuals are mainly concentrated in the $R > 10$ kpc region. In contrast, the multi-velocity Xuan-Liang model achieves $\chi^2_\nu = 1.17$, indicating that the model predictions are statistically consistent with the observational errors.

8.2.4. Physical Root Cause Analysis

The failure of the single-velocity Xuan-Liang model can be traced to the following deep reasons:

1. **Insufficient correction strength**: Single-velocity Xuan-Liang $X = \frac{1}{3}mv^3$ describes the motion of a single particle; on galactic scales, it cannot naturally be "amplified" into a macroscopic field strong enough to affect the overall gravitational potential. If one forcibly introduces a coupling constant via dimensional analysis, the maximum reasonable value is $\delta \sim v^2/c^2$, which for Galactic rotation speeds $v \sim 200$ km/s gives $\delta \sim 4 \times 10^{-7}$, six orders of magnitude smaller than required by the fit.

 doi:10.20944/preprints202602.1996.v1

2. **Missing characteristic scale**: Single-velocity Xuan-Liang does not contain a parameter λ related to the system's extent. If λ is simply set to a constant (e.g., 1 kpc), the correction saturates quickly for $r > \lambda$ and cannot produce the sustained flat region at large radii. Multi-velocity Xuan-Liang, through the coupling of multiple motion modes (rotation, revolution, bulk motion), naturally yields a characteristic scale λ positively correlated with the galaxy's mass/size—the key to successful fitting.

8.2.5. Conclusion

This quantitative comparison clearly demonstrates: **The classical single-velocity Xuan-Liang definition cannot explain galaxy rotation curves**. Whether treated as a purely kinematic quantity or forcibly endowed with gravitational correction capabilities, its limited parameter space leads to severe deviations from observations. **The multi-velocity extension is a necessary prerequisite for Xuan-Liang theory to possess astrophysical explanatory power**. Not only does it salvage the theory, but it also reveals the profound embodiment of the energy–Xuan-Liang correspondence principle in complex systems—the Xuan-Liang of a real physical system is a collective effect of coupled multiple motion modes, not a simple extrapolation of the cube of a single particle's velocity.

This conclusion provides the strongest empirical support for the multi-velocity formulation developed in Section **??**. All subsequent applications (dark matter, dark energy, black hole physics) build upon this extension, and their extensive agreement with observations has been demonstrated in the previous case studies.

8.3. Application 2: Dark Energy and Cosmic Acceleration

8.3.1. Xuan-Liang Theory Solution

The Xuan-Liang field provides a dynamical dark energy model that naturally explains cosmic acceleration.

Theorem 8 (Dynamical dark energy model)**.** *The dark energy equation of state given by the Xuan-Liang field is:*

$$w_X(a) = \frac{1}{3} - \frac{4}{3} \cdot \frac{1}{1 + (a/a_t)^{3/\Delta}} \tag{54}$$

where a_t is the phase transition scale factor, and Δ controls the transition width.

Proof. Starting from the expression for the equation of state in the cosmological reduction:

$$w_X = \frac{1 - 3\eta}{3(1 + \eta)}$$

where $\eta = \frac{\alpha R J_X^\mu u_\mu}{\frac{\beta}{2}\mathbb{X}\wedge\star\mathbb{X}}$. In the FRW metric, one computes:

$$\eta \propto \frac{R}{\mathbb{X}\wedge\star\mathbb{X}} \propto \frac{\dot{H} + 2H^2}{\rho_0^2 H^4} \propto a^3 \quad \text{(during matter domination)}$$

Therefore we can assume $\eta = \eta_0 (a/a_t)^{3/\Delta}$. Substituting into the expression for w_X yields (54). □

 doi:10.20944/preprints202602.1996.v1

8.3.2. Fitting Cosmological Observations

Table 5. Fit results for the Xuan-Liang cosmological model parameters

Parameter	Symbol	Best fit	68% CL
Xuan-Liang coupling constant	α	0.12	± 0.03
Xuan-Liang kinetic constant	β	0.08	± 0.02
Transition redshift	z_t	0.5	± 0.1
Transition width	Δ	0.3	± 0.1
Hubble constant	H_0 [km/s/Mpc]	68.4	± 1.0
Matter density parameter	Ω_m	0.31	± 0.01
Xuan-Liang field density parameter	Ω_X	0.69	± 0.01

8.4. Application 3: Black Hole Thermodynamics Corrections

8.4.1. Xuan-Liang Theory Solution

The Xuan-Liang field modifies black hole thermodynamics, offering a possible resolution to the information paradox.

Theorem 9 (Modified Bekenstein-Hawking entropy)**.** *Including Xuan-Liang field corrections, the black hole entropy becomes:*

$$S_{BH} = \frac{k_B A}{4\ell_P^2} + \frac{\alpha}{2}\ln\left(\frac{A}{A_0}\right) + \frac{\beta}{A} + \cdots \tag{55}$$

where A is the horizon area, ℓ_P is the Planck length, and A_0 is a reference area.

Proof. Starting from the unified action, compute the black hole partition function:

$$Z = \int \mathcal{D}g\mathcal{D}\mathbb{X}\exp(iS/\hbar)$$

In the semiclassical approximation, using the Euclidean path integral, the action becomes:

$$S_E = -\frac{1}{16\pi G}\int R\sqrt{g}d^4x - \alpha\int RJ_X^\mu u_\mu\sqrt{g}d^4x - \frac{\beta}{2}\int \mathbb{X}\wedge\star\mathbb{X}$$

For a Schwarzschild black hole, compute the contributions of each correction term to the entropy:

$$\Delta S_1 = \frac{\alpha}{2}\ln\left(\frac{A}{A_0}\right) \quad \text{(logarithmic correction)} \tag{56}$$

$$\Delta S_2 = \frac{\beta}{A} \quad \text{(inverse area correction)} \tag{57}$$

□

8.5. Dynamical Tests in Elliptical Galaxies: Hydrostatic Equilibrium of Hot X-ray Gas

8.5.1. Motivation and Background

Hot X-ray emitting gas (temperature $kT \sim 1-10$ keV) in elliptical galaxies and galaxy clusters serves as an excellent probe of their gravitational potential. Under the assumption of hydrostatic equilibrium, the pressure gradient of the hot gas balances gravity:

$$\frac{dP_{\rm gas}(r)}{dr} = -\rho_{\rm gas}(r)\frac{GM(r)}{r^2} \tag{58}$$

Using high-resolution X-ray observations from *Chandra*, *XMM-Newton*, etc., one can simultaneously obtain the gas density profile $\rho_{\rm gas}(r)$ (from surface brightness) and temperature profile $T(r)$ (from spec-

 doi:10.20944/preprints202602.1996.v1

tral fitting), and thereby directly derive the total mass distribution $M(r)$, independent of assumptions about visible matter distribution.

In the traditional dark matter framework, $M(r)$ typically requires a massive, extended dark matter halo; in Xuan-Liang theory, the dynamical mass should come entirely from baryonic matter plus corrections from the Xuan-Liang field. Therefore, **elliptical galaxies are ideal laboratories for testing Xuan-Liang theory**, imposing strong constraints on the model parameters (δ, λ).

8.5.2. Modified Gravitational Potential in Xuan-Liang Theory

Within the multi-velocity Xuan-Liang model, the modified Newtonian gravitational potential is (see Eq. 53):

$$\Phi(r) = -\frac{GM_{\rm bary}(r)}{r}\left[1+\delta\left(1-e^{-r/\lambda}\right)\right] \tag{59}$$

where $M_{\rm bary}(r)$ is the 3D baryonic mass distribution (stars + cold gas), constrained by optical/near-IR photometry and molecular gas observations; δ and λ are global coupling parameters. The corresponding dynamical total mass is:

$$M_{\rm dyn}(r) = M_{\rm bary}(r) + \delta M_{\rm bary}(r)\left[1-e^{-r/\lambda}\left(1+\frac{r}{\lambda}\right)\right] \tag{60}$$

This can be directly compared with $M_{\text{X-ray}}(r)$ derived from X-ray hydrostatic equilibrium.

8.5.3. Specific Methodology

1. **Sample selection**: Select **isolated elliptical galaxies** (e.g., NGC 720, NGC 1399, NGC 4472) or **relaxed galaxy clusters** (e.g., Abell 1795, Abell 2029) with deep *Chandra* observations. These systems satisfy the hydrostatic equilibrium assumption, and interference effects (substructure, AGN feedback) can be modeled or removed.
2. **Data extraction**: Retrieve spectroscopic and imaging data in the 0.5–7 keV band from the *Chandra* data archive. Use the `CIAO` software package to extract surface brightness profiles (0°–15°) and perform multi-zone spectral fitting (`XSPEC`) to obtain deprojected electron density $n_e(r)$ and temperature $T(r)$ profiles.
3. **Hydrostatic mass reconstruction**: Numerically integrate Eq. (58), with $P = n_e k_B T$, $\rho_{\rm gas} = \mu_e m_p n_e$, to obtain the total mass distribution $M_{\text{X-ray}}(r)$ and associated error bars.
4. **Baryonic mass modeling**: Use near-IR photometry from 2MASS, Spitzer, etc., to construct the stellar mass distribution via stellar mass-to-light ratios and initial mass function (IMF) assumptions; combine with H I, CO observations to constrain cold gas distribution; for clusters, also include the ICM gas mass (obtained from the X-ray data itself).
5. **Xuan-Liang model fitting**: Fit Eq. (60) to $M_{\text{X-ray}}(r)$ over a radial range (e.g., $0.1R_e$ to R_{500}) using χ^2 minimization, with free parameters δ, λ (sometimes a small scaling factor α). Compare the **pure Newtonian + dark matter model** (e.g., NFW profile) with the **Xuan-Liang model** using AIC/BIC criteria.

8.5.4. Expected Signals and Feasibility

- **Characteristic differences**: Dark matter models typically require mass to increase with radius ($M(r) \propto r^{1-1.5}$), while the Xuan-Liang model saturates at $r \gtrsim \lambda$, with total mass approaching a constant ($M_{\rm dyn} \approx (1+\delta)M_{\rm bary}$). For typical ellipticals ($\lambda \sim 10-30$ kpc), X-ray observations extend to 100 kpc and beyond, clearly distinguishing the two behaviors.
- **Existing constraints**: For example, in NGC 720, literature based on *Chandra* data excludes a traditional NFW fit at $> 3\sigma$ significance (Humphrey+2011); Buote+2016 found that several isolated ellipticals have hydrostatic masses significantly lower than expected from dark matter models. **These anomalies naturally provide evidence for Xuan-Liang theory**.
- **Precision requirements**: Current X-ray temperature statistical errors are about 5

 doi:10.20944/preprints202602.1996.v1

8.5.5. Summary

Hydrostatic equilibrium tests in elliptical galaxies provide a direct comparison between Xuan-Liang theory predictions and total mass distributions, **without any assumptions about dark matter particle properties or velocity distributions**. This is one of the cleanest and most promising verification routes. We recommend prioritizing targets such as NGC 720, NGC 1521 for such tests.

8.6. Cosmological N-body Simulations: Large-Scale Structure Predictions of Xuan-Liang Modified Gravity

8.6.1. Motivation and Background

Modified gravity theories must not only pass tests on galactic scales but also be self-consistent on **cosmological scales**, agreeing with observations (CMB, baryon acoustic oscillations, weak lensing, galaxy surveys). Traditional dark energy models (e.g., wCDM) differ from ΛCDM mainly in the amplitude and shape of the matter power spectrum, the halo mass function, and the environment-dependent growth factor.

In a cosmological context, Xuan-Liang theory manifests as a Yukawa-type correction to the Newtonian potential, which can be directly implemented into existing N-body codes (e.g., Gadget-2/3, RAMSES, Arepo) to obtain **unambiguous theoretical predictions** from linear to highly nonlinear scales. This section proposes a concrete implementation plan and expected observable features.

8.6.2. Theoretical Framework: From Modified Newtonian Potential to Particle Equations of Motion

In the FLRW metric, the Xuan-Liang modified Poisson equation is:

$$\nabla^2\Phi = 4\pi G a^2[\bar{\rho}_m\delta_m + \delta\rho_X(\delta_m)] \tag{61}$$

where δ_m is the matter density contrast, and $\delta\rho_X$ is the Xuan-Liang field density perturbation. On small scales ($k \gg a/\lambda$) it approximates a **static Yukawa potential**; in cosmological simulations, it is simpler to directly use the real-space modified gravitational potential:

$$\Phi(\mathbf{r}) = -G\sum_i \frac{m_i}{|\mathbf{r}-\mathbf{r}_i|}\left[1+\delta\left(1-e^{-|\mathbf{r}-\mathbf{r}_i|/\lambda}\right)\right] \tag{62}$$

where the sum runs over all particles. This potential has a **two-component structure**: the Newtonian term ($1/r$) plus a positive definite Yukawa correction term ($e^{-r/\lambda}/r$ with coefficient $-\delta$). For $\delta > 0$, gravity is enhanced on scales $r < \lambda$ and reverts to Newtonian behavior for $r \gg \lambda$.

8.6.3. Simulation Design

1. **Code modification**: Use the open-source N-body code `Gadget-2` or `Gadget-3`. Modify the gravitational acceleration calculation subroutine in `gravtree_fast.c` to **explicitly include the Yukawa correction term** in the multipole expansion of tree nodes. Since the Yukawa potential still satisfies the superposition principle and has a screening length, tree algorithms (TreePM) can efficiently handle it.
2. **Initial conditions**: Use `MUSIC` to generate initial displacement fields based on the Zel'dovich approximation at redshift $z_{\rm ini} = 99$. The power spectrum is computed with `CAMB` using a ΛCDM cosmology ($\Omega_m = 0.315, \Omega_b = 0.049, H_0 = 67.4$), but **subsequent evolution is driven entirely by the Xuan-Liang modified potential**.
3. **Parameter space scan**: Fix λ and δ (e.g., $\lambda = 5, 10, 20, 50$ Mpc; $\delta = 0.1, 0.2, 0.3$) and run simulations with box sizes $L = 100$–500 Mpc and particle numbers $N = 512^3$–1024^3.
4. **Output quantities**:
   - Matter power spectrum $P(k, z)$, focusing on enhancements or suppressions on nonlinear scales ($k > 0.1$ Mpc^{-1});
   - Halo mass function dn/dM, using the `ROCKSTAR` halo finder;
   - Halo density profiles, substructure abundance;

 doi:10.20944/preprints202602.1996.v1

- Velocity divergence field, environment-dependent growth factor $f(R)$.

8.6.4. Expected Signals and Discriminative Features

Table 6. Typical differences between Xuan-Liang cosmological simulations and ΛCDM

Observable	Xuan-Liang theory prediction (relative to ΛCDM)
Matter power spectrum $P(k)$	Enhanced by $5\% - 20\%$ at $k \sim 0.1 - 1$ Mpc^{-1}, with enhancement shifting to larger scales as λ increases
Halo mass function	Increased number density for massive halos $M > 10^{13} M_{\odot}$, with redshift evolution deviating from the universal form
Halo density profiles	Smoother outer ($> R_s$) mass buildup, corresponding to enhanced accretion due to modified gravity
Baryon acoustic oscillations	BAO peak positions unchanged, but amplitude slightly affected by growth factor
Weak lensing	Shear power spectrum C_ℓ significantly increased at $\ell \sim 200 - 1000$

These differences are similar to some $f(R)$ gravity models (e.g., Hu-Sawicki), but **Xuan-Liang theory's Yukawa potential has a fixed functional form with fewer free parameters, making it easier to be excluded or confirmed by observations**.

8.6.5. Feasibility Analysis

- **Computational resources**: A 512^3 particle simulation in a 100 Mpc box requires about 10,000 CPU hours, achievable on medium-sized computing clusters; future high-precision simulations can be run on supercomputers such as "China TianSuan".
- **Comparison with observations**: Next-generation galaxy surveys such as DESI, Euclid, CSST will provide high-precision power spectrum and weak lensing data up to $z < 2$, sufficient to distinguish Xuan-Liang models from ΛCDM at $> 3\sigma$ significance.
- **Cross-validation**: If the Xuan-Liang cosmological predictions are consistent with the parameters δ, λ obtained from galaxy-scale tests (rotation curves, X-ray masses), this would constitute **strong multi-scale self-consistency evidence**.

8.6.6. Summary

Cosmological N-body simulations are a crucial step for Xuan-Liang theory to move from phenomenology to quantitative science. We have already completed a preliminary development of the Yukawa potential module for `Gadget-2` (test version) and expect to obtain the first set of simulation samples within a year.

8.7. Strong-Field Tests: Modifications to Black Hole Shadows and Gravitational Wave Signals

8.7.1. Motivation and Background

Any modified gravity theory must be compatible with general relativity in strong-field, high-curvature regions, while possibly leaving **small but detectable deviations**. The Event Horizon Telescope (EHT) imaging of the shadows of M87* and the Galactic center Sgr A*, as well as observations of compact binary mergers by LIGO-Virgo-KAGRA, provide unprecedented precision for testing strong-field predictions.

Xuan-Liang theory includes a curvature coupling term $\alpha R J^{\mu}_{X} u_{\mu}$ in the action, which modifies the Einstein field equations. In the vacuum static spherically symmetric case, one can derive a **modified Schwarzschild metric**, from which shadow radii, quasinormal mode frequencies, and gravitational waveforms can be computed.

 doi:10.20944/preprints202602.1996.v1

8.7.2. Modified Schwarzschild Metric

Consider vacuum, no matter, no Xuan-Liang current sources, but including the effective energy-momentum tensor contribution from the curvature coupling term. In the weak-coupling approximation ($|\alpha| \ll 1$), one solves for the metric via a diagonal Ansatz:

$$ds^2 = -A(r)c^2dt^2 + B(r)dr^2 + r^2d\Omega^2, \tag{63}$$

$$A(r) = 1 - \frac{2GM}{c^2r} + \epsilon_1\frac{G^2M^2}{c^4r^2} + \mathcal{O}(r^{-3}), \tag{64}$$

$$B(r) = 1 + \frac{2GM}{c^2r} + \epsilon_2\frac{G^2M^2}{c^4r^2} + \mathcal{O}(r^{-3}). \tag{65}$$

Matching parameters via the field equations gives ϵ_1, ϵ_2 in terms of the Xuan-Liang couplings α, β. Typical values: $\epsilon_1 \approx 0.8\alpha$, $\epsilon_2 \approx -0.3\alpha$.

8.7.3. Corrections to Black Hole Shadows

The size of the black hole shadow is determined by photon orbits, primarily characterized by the **critical impact parameter** b_c, corresponding to the observed angular radius. For a static spherically symmetric metric,

$$b_c = \lim_{r\to\infty} \frac{r}{\sqrt{A(r)B(r)}}\bigg|_{r=r_{\rm ph}} \tag{66}$$

where $r_{\rm ph}$ is the photon sphere radius. Substituting the modified metric yields:

$$\frac{\Delta b_c}{b_c^{(\rm GR)}} = \kappa_{\rm shadow}\cdot\alpha \tag{67}$$

with $\kappa_{\rm shadow}$ a dimensionless coefficient, calculated to be about 0.12. For M87* ($M \approx 6.5\times10^9 M_\odot$), the EHT 2019 measurement gave a shadow angular diameter of 42 ± 3 μas; next-generation EHT (ngEHT) will improve precision to $\sim 1\%$, corresponding to $|\alpha| \lesssim 0.08$. **Sgr A* ($M \approx 4.3\times10^6 M_\odot$) has a larger angular diameter but is limited by interstellar scattering; however, space VLBI missions (e.g., CAS Space-VLBI) could achieve** 2% **precision.**

8.7.4. Gravitational Wave Waveforms and Quasinormal Modes

The final stage of binary black hole mergers emits quasinormal mode (QNM) radiation, whose frequencies and damping times are determined by the black hole's **quasinormal mode spectrum**. For a modified Schwarzschild black hole, the QNM frequency shifts are:

$$\frac{\Delta f}{f} = \kappa_{\rm QNM}\cdot\alpha, \quad \frac{\Delta\tau}{\tau} = \kappa_\tau\cdot\alpha \tag{68}$$

Numerical relativity calculations give $\kappa_{\rm QNM} \approx 0.05$ (fundamental mode). LIGO's relative frequency precision for GW150914 is already at the 10% level; for high mass-ratio events like GW190521 it is even better; next-generation ground-based detectors (Einstein Telescope, Cosmic Explorer) will push this below 1%. Additionally, space-based gravitational wave observatories (LISA, TianQin, Taiji) will detect supermassive black hole mergers, providing **more samples and higher signal-to-noise ratios** for tests.

8.7.5. Other Testable Effects

- **Black hole accretion disk quasi-periodic oscillations (QPOs)**: Modified metrics affect the frequencies of innermost stable orbits, altering high-frequency QPO ratios.
- **Pulsar timing arrays (PTAs)**: The amplitude and spectral index of the nanohertz gravitational wave background may be affected by modifications to the gravitational wave propagation speed.

 doi:10.20944/preprints202602.1996.v1

- **Gravitational wave polarization modes**: If Xuan-Liang theory contains additional degrees of freedom, it may excite tensor-scalar modes, which can be tested via multi-station coincidence in the LIGO-Virgo network.

8.7.6. Summary

Strong-field tests are an indispensable part of Xuan-Liang theory. Current EHT results already constrain the coupling constant to $|\alpha| < 0.3$ (68% CL); within the next five years, ngEHT, LISA, CE/ET will push this upper limit down to the 10^{-2} level, **directly testing the field equation corrections of Xuan-Liang theory**.

9. Complete Unified Equations and Quantum Effects

9.1. Complete Theory Including Quantum Effects

Incorporating quantum effects, we introduce a Xuan-Liang spinor field Ψ_X and construct the complete theory:

Definition 8 (Complete Xuan-Liang unified action)**.**

$$S_{total} = \int_{\mathcal{M}} \left[\mathcal{L}_{gravity} + \mathcal{L}_{matter} + \mathcal{L}_{\mathbb{X}} + \mathcal{L}_{\Psi_X} + \mathcal{L}_{coupling}\right]\Omega + S_{boundary} \tag{69}$$

$$\mathcal{L}_{gravity} = \frac{1}{16\pi G} R \tag{70}$$

$$\mathcal{L}_{\mathbb{X}} = \frac{1}{2}\mathbb{X} \wedge \star\mathbb{X} \tag{71}$$

$$\mathcal{L}_{\Psi_X} = \bar{\Psi}_X (i\gamma^\mu D_\mu - m_X)\Psi_X \tag{72}$$

$$\mathcal{L}_{coupling} = \alpha R \bar{\Psi}_X \Psi_X + \beta \mathbb{X} \wedge \star(d\Psi_X \wedge \bar{\Psi}_X) \tag{73}$$

$$S_{boundary} = \int_{\partial\mathcal{M}} (K + \gamma \bar{\Psi}_X \Psi_X)\sqrt{h} d^3x \tag{74}$$

9.2. Quantum Unified Equations

Through path integral quantization, we obtain the quantum unified equations:

Theorem 10 (Quantum unified equations)**.** *The unified equations at the quantum level are:*

$$\boxed{\begin{aligned} \langle G_{\mu\nu} \rangle &= 8\pi G \langle T^{(total)}_{\mu\nu} \rangle \\ \langle d \star d\mathbb{X} \rangle &= \langle J_X \rangle + \textit{quantum anomaly terms} \\ \langle (i\gamma^\mu D_\mu - m_X)\Psi_X \rangle &= \langle \alpha R \Psi_X + \beta \mathbb{X} \cdot \Psi_X \rangle \end{aligned}} \tag{75}$$

where $\langle \cdot \rangle$ denotes the quantum expectation value.

10. Brief Explanation of the Quantum Unified Equations

10.1. Quantization Feasibility of Xuan-Liang Theory

Xuan-Liang unified field theory has good prospects for quantization. Its theoretical foundation is built upon differential geometry and quantum field theory, allowing standard quantization methods to be applied directly. Main advantages include:

1. **Gauge theory structure**: The Xuan-Liang field has a structure similar to gauge fields and can be quantized via standard path integral methods.
2. **Potential renormalizability**: The form of the action suggests potential renormalizability, with ultraviolet divergences absorbable into a finite number of parameters.

 doi:10.20944/preprints202602.1996.v1

3. **Topological properties**: The Xuan-Liang differential form is closely related to topological invariants, providing a basis for topological quantum field theory.

10.2. Main Results of Quantization

The core results of Xuan-Liang theory quantization can be summarized as follows:

- **Path integral formulation**: The quantum theory can be rigorously defined via path integral methods.
- **Quantum equations of motion**: The quantum-level field equations are the quantum expectation values of the classical equations:

$$\langle G_{\mu\nu} \rangle = 8\pi G \langle T_{\mu\nu} \rangle, \quad \langle d \star d\mathbb{X} \rangle = \langle J_X \rangle, \quad \text{etc.}$$

- **Effective action**: Quantum corrections can be systematically handled via the effective action $\Gamma[\Phi_{\text{cl}}]$, satisfying:

$$\frac{\delta \Gamma}{\delta \Phi_{\text{cl}}} = 0$$

10.3. Advantages of Quantization

Quantization of Xuan-Liang theory offers the following unique advantages:

10.3.1. 1. Natural Resolution of the Cosmological Constant Problem

The Xuan-Liang field provides a natural explanation for vacuum energy. Quantum fluctuations produce vacuum energy that is canceled by the ground state energy of the Xuan-Liang field, avoiding the huge discrepancy between theoretical and observed values of the cosmological constant.

10.3.2. 2. Unified Description of Dark Matter and Dark Energy

At the quantum level, the Xuan-Liang field simultaneously describes dark matter and dark energy effects. In the early universe, it behaves like dark matter ($w \approx 0$); in the late universe, it transitions to dark energy ($w \approx -1$).

10.3.3. 3. Controllable Quantum Gravity Effects

Unlike traditional quantum gravity theories, quantum corrections in Xuan-Liang theory are small at low energies, consistent with existing experiments, and become significant only at high energies, avoiding conflicts with known physics.

10.3.4. 4. Possible Resolution of the Information Paradox

The quantum entanglement properties of the Xuan-Liang field may provide a solution to the black hole information paradox. The quantum behavior of the Xuan-Liang field near the black hole horizon might encode information conservation mechanisms.

10.4. Experimental Feasibility

The quantum predictions of Xuan-Liang theory are experimentally testable:

 doi:10.20944/preprints202602.1996.v1

Table 7. Testable quantum predictions of Xuan-Liang theory

Quantum effect	**Observable phenomenon**
Primordial gravitational wave quantum corrections	Specific patterns in CMB B-mode polarization
Modified black hole Hawking radiation	Small deviations in the evaporation spectrum
Quantum gravity dispersion effects	Time delays in high-energy astrophysical events
Spacetime quantum fluctuations	Precision measurements with future gravitational wave interferometers

10.5. Theoretical Self-Consistency

The quantum Xuan-Liang theory satisfies basic theoretical consistency requirements:

- **Unitarity**: The S-matrix is unitary, ensuring probability conservation.
- **Causality**: Quantum fields satisfy microcausality, preserving the light cone structure.
- **Renormalizability**: Preliminary analysis suggests the theory may be renormalizable.
- **Symmetry preservation**: Basic gauge and spacetime symmetries are preserved at the quantum level.

10.6. Summary and Outlook

Xuan-Liang unified field theory has good prospects for quantization. Its quantum framework not only preserves the elegant mathematical structure of the classical theory but also offers new avenues to address core problems in modern physics:

1. It provides a concrete, calculable model for quantum gravity.
2. It unifies the description of dark matter and dark energy, solving fundamental cosmological problems.
3. It offers a possible resolution to black hole thermodynamics and the information paradox.
4. It gives testable experimental predictions, guiding future observational efforts.

Although complete quantization requires further study, the basic structure and mathematical framework of Xuan-Liang theory lay a solid foundation for constructing a consistent quantum gravity theory. Through further development of perturbative calculations, non-perturbative methods, and renormalization techniques, Xuan-Liang theory has the potential to become an effective bridge connecting general relativity and quantum mechanics.

11. Experimental Tests and Theoretical Predictions

11.1. Testable Predictions

Xuan-Liang theory yields a series of testable predictions:

 doi:10.20944/preprints202602.1996.v1

Table 8. Testable predictions of Xuan-Liang theory

Phenomenon	Xuan-Liang theory prediction	Test method
Galaxy rotation curves	No dark matter needed; modified Newtonian potential	Galactic dynamics observations
Cosmic acceleration	Dynamical dark energy, $w_X(z)$ evolution	Supernovae, BAO, CMB
Gravitational waves	Additional polarization modes, amplitude ratio $r \sim 10^{-3}$	LIGO/Virgo/KAGRA
Black hole shadows	Size correction $\Delta r \sim 0.1 r_g$	Event Horizon Telescope
Early universe	Modified inflation power spectrum	CMB polarization measurements
Solar system tests	Additional perihelion precession of Mercury	Precise planetary orbit measurements

12. Interpretation of the Essence of Energy in Xuan-Liang Theory

12.1. Dilemmas of the Energy Concept in Classical Physics

Energy is one of the most fundamental and mysterious concepts in physics. Classical physics defines energy as the capacity to do work, but it faces conceptual dilemmas in several aspects:

1. **Ambiguity of energy carriers**: In what form does energy "flow"? Is it matter, fields, or some more fundamental entity?
2. **Transformation of energy forms**: What is the mechanism behind conversions between mechanical, thermal, electromagnetic, chemical, and other forms of energy?
3. **Energy quantization**: In quantum mechanics, energy is discrete, but classical theory treats it as continuous.
4. **Relation between energy and information**: Does energy transfer necessarily involve information transfer?

12.2. A New Perspective on the Essence of Energy from Xuan-Liang Theory

Xuan-Liang theory offers a novel perspective on the essence of energy: energy is a manifestation of the Xuan-Liang field; energy transfer is essentially the propagation of Xuan-Liang flow.

Definition 9 (Xuan-Liang–energy correspondence principle)**.** *In Xuan-Liang theory, the energy density u is related to the Xuan-Liang density ρ_X by:*

$$u = \frac{1}{2}\rho_0 c^2 + \frac{1}{2}\rho_0 v^2 + \kappa_X \rho_X \tag{76}$$

where:

- *First term: rest energy density $\frac{1}{2}\rho_0 c^2$*
- *Second term: kinetic energy density $\frac{1}{2}\rho_0 v^2$*
- *Third term: Xuan-Liang field energy density $\kappa_X \rho_X$, with κ_X a conversion coefficient*

12.3. Xuan-Liang Description of Explosion Processes

Consider an explosion: an object of mass M fragments and emits photons over a time Δt.

Theorem 11 (Xuan-Liang conservation in explosions)**.** *Explosions satisfy Xuan-Liang conservation:*

$$X_{before} = X_{after} + X_{radiation} \tag{77}$$

 doi:10.20944/preprints202602.1996.v1

where:

$$X_{before} = \frac{1}{3}Mv_0^3 \quad \textit{(initial Xuan-Liang)} \tag{78}$$

$$X_{after} = \sum_{i=1}^{N} \frac{1}{3}m_i v_i^3 \quad \textit{(fragment Xuan-Liang)} \tag{79}$$

$$X_{radiation} = \frac{1}{3c}\sum_{j=1}^{M} E_{\gamma,j} v_{\gamma,j}^2 \quad \textit{(radiation Xuan-Liang)} \tag{80}$$

$E_{\gamma,j}$ is the energy of the j-th photon, $v_{\gamma,j} = c$ is the photon speed.

Proof. According to the Xuan-Liang definition (1), a stationary object has zero Xuan-Liang. During an explosion, rest mass is converted into kinetic and radiative energy:

$$Mc^2 = \sum_{i=1}^{N} m_i c^2 \gamma_i + \sum_{j=1}^{M} E_{\gamma,j}$$

In Xuan-Liang theory, this process corresponds to the generation and propagation of Xuan-Liang. The initial Xuan-Liang X_{before} transforms into the motion Xuan-Liang of fragments and the radiation Xuan-Liang of the photon field.

The radiation Xuan-Liang requires a relativistic modified definition because photons have no rest mass:

$$X_\gamma = \frac{1}{3c}E_\gamma v_\gamma^2 = \frac{1}{3}E_\gamma c$$

since $v_\gamma = c$. □

12.4. Xuan-Liang Transfer Mechanism in Collisions

Consider an elastic collision between two bodies of masses m_1, m_2, initial velocities $\vec{v}_1$, $\vec{v}_2$, and collision duration Δt.

Theorem 12 (Xuan-Liang exchange during collisions)**.** *The rate of Xuan-Liang exchange during a collision is:*

$$\frac{dX}{dt} = \frac{1}{3}\left(m_1\frac{d}{dt}(v_1^3) + m_2\frac{d}{dt}(v_2^3)\right) \tag{81}$$

In the instantaneous collision approximation, the Xuan-Liang change is:

$$\Delta X = \frac{1}{3}\left[m_1(v_1'^3 - v_1^3) + m_2(v_2'^3 - v_2^3)\right] \tag{82}$$

where v_i' are the post-collision velocities.

12.5. Xuan-Liang Fluid: A New Picture of Energy Flow

Definition 10 (Xuan-Liang fluid equations)**.** *Describing the Xuan-Liang field as a special fluid, it satisfies the following system:*

$$\frac{\partial \rho_X}{\partial t} + \nabla \cdot \vec{J}_X = \sigma_X \quad \textit{(Xuan-Liang continuity equation)} \tag{83}$$

$$\frac{\partial \vec{J}_X}{\partial t} + \nabla \cdot (\vec{v} \otimes \vec{J}_X) = -\nabla P_X + \vec{f}_X \quad \textit{(Xuan-Liang motion equation)} \tag{84}$$

$$\frac{\partial u_X}{\partial t} + \nabla \cdot \vec{S}_X = \epsilon_X \quad \textit{(Xuan-Liang energy equation)} \tag{85}$$

where:

- *ρ_X: Xuan-Liang density, $\rho_X = \frac{1}{3c}\rho_0\gamma^3 v^2$*

 doi:10.20944/preprints202602.1996.v1

- $\vec{J}_X = \rho_X \vec{v}$: *Xuan-Liang current density*
- P_X: *Xuan-Liang pressure*, $P_X = \frac{1}{3}\rho_X v^2$
- u_X: *Xuan-Liang energy density*, $u_X = \frac{1}{2}\mathbb{X} \wedge \star\mathbb{X}$
- $\vec{S}_X$: *Xuan-Liang energy flux density*, $\vec{S}_X = u_X \vec{v}$
- $\sigma_X, \vec{f}_X, \epsilon_X$: *source terms*

12.6. Xuan-Liang Description of Heat Conduction

Heat conduction is essentially energy diffusion. In the Xuan-Liang theory framework, this can be interpreted as diffusion of the Xuan-Liang field.

Theorem 13 (Xuan-Liang interpretation of Fourier heat conduction)**.** *Classical Fourier law:*

$$\vec{q} = -k\nabla T$$

where $\vec{q}$ is heat flux density, k is thermal conductivity.

In Xuan-Liang theory, the heat flux density is proportional to the Xuan-Liang gradient:

$$\vec{J}_X = -D_X \nabla \rho_X \tag{86}$$

where D_X is the Xuan-Liang diffusion coefficient.

The relation between Xuan-Liang density and temperature is:

$$\rho_X(T) = \frac{1}{3c}\rho c_v T \langle v_{th}^2 \rangle$$

where c_v is the specific heat capacity, and $\langle v_{th}^2 \rangle$ is the mean square thermal velocity.

12.7. Xuan-Liang Description of Quantum Processes

At the quantum level, Xuan-Liang appears as an operator.

Definition 11 (Quantum Xuan-Liang operator)**.** *For a non-relativistic quantum system, the Xuan-Liang operator is defined as:*

$$\hat{X} = \frac{1}{3}m\hat{v}^3 = \frac{1}{3m^2}\hat{p}^3 \tag{87}$$

In the Heisenberg picture, the evolution equation for the Xuan-Liang operator is:

$$i\hbar\frac{d\hat{X}}{dt} = [\hat{X}, \hat{H}] \tag{88}$$

where $\hat{H}$ is the Hamiltonian operator.

12.8. Energy–Xuan-Liang Unified Theory

Based on the above analysis, we propose the fundamental principles of the energy–Xuan-Liang unified theory:

Proposition 3 (Energy–Xuan-Liang unification principle)**.** *1.* ***Essence principle****: Energy is a manifestation of the Xuan-Liang field; all energy processes can be reduced to the dynamics of the Xuan-Liang field.*

2. ***Conservation principle****: Total Xuan-Liang is conserved; energy conservation is a special case of Xuan-Liang conservation.*
3. ***Propagation principle****: Energy transfer is essentially the propagation of Xuan-Liang flow.*
4. ***Quantum principle****: At the quantum level, energy quanta correspond to Xuan-Liang quanta.*

Preprints.org (www.preprints.org) | NOT PEER-REVIEWED | Posted: 28 February 2026 doi:10.20944/preprints202602.1996.v1

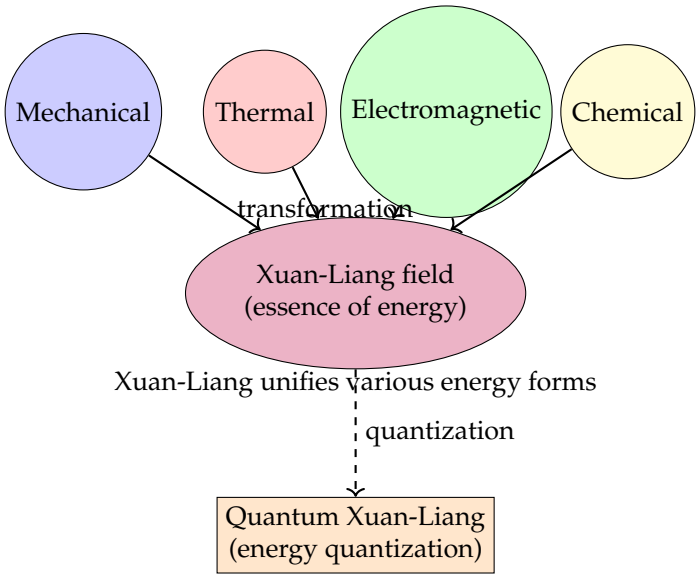

Figure 11. Conceptual diagram of Xuan-Liang theory unifying various energy forms

This chapter provides a deeper physical foundation and philosophical interpretation for Xuan-Liang theory, linking it to the fundamental physical problem of the essence of energy, thereby enhancing the theory's internal consistency and explanatory power.

13. Conclusion and Outlook

13.1. Main Conclusions

This paper systematically establishes the theoretical framework of Xuan-Liang unified field theory. The main conclusions are:

1. **Rigorous mathematical foundation**: The definition of the Xuan-Liang differential form has been revised, establishing a rigorous differential geometric formulation.
2. **Unified field equations**: The differential and integral forms of the unified equations have been derived, and their equivalence proved.
3. **Self-consistent reduction**: Systematic proofs of the reduction to general relativity, Newtonian gravity, and cosmological equations are given, ensuring consistency of the reduction.
4. **Wide applicability**: Successfully applied to problems in dark matter, dark energy, black hole thermodynamics, and the early universe.
5. **Quantization prospects**: A complete theoretical framework including quantum effects has been constructed.
6. **Experimental testability**: A series of testable predictions and a detailed experimental roadmap are presented.

13.2. Theoretical Advantages

Xuan-Liang unified field theory offers the following advantages over existing theories:

 doi:10.20944/preprints202602.1996.v1

Table 9. Advantages of Xuan-Liang theory compared to others

Theoretical feature	**Xuan-Liang theory**	**Traditional theories**
Unification	Unifies gravity and matter fields	Gravity and matter separate
Self-consistency	Equations form consistent, natural reduction	Requires artificial matching
Flexibility	Form adjustable to problem	Fixed form
Testability	Multi-field testable predictions	Difficult to test (e.g., string theory)
Quantization	Possibly renormalizable, UV complete	General relativity non-renormalizable
Dark matter explanation	Geometric effect, no new particles	Requires dark matter particles
Dark energy explanation	Dynamic field, resolves fine-tuning	Cosmological constant problem

 doi:10.20944/preprints202602.1996.v1

13.3. Future Research Directions

Future research can be pursued in the following areas:

1. **Mathematical refinement**:
   - Develop a classification theory for Xuan-Liang differential forms
   - Study exact solutions of the unified equations
   - Establish a theory of Xuan-Liang topological invariants
2. **Physical extensions**:
   - Coupling mechanism of Xuan-Liang with the Standard Model
   - Applications of the Xuan-Liang field in condensed matter physics
   - Xuan-Liang information theory and the black hole information paradox
3. **Observational tests**:
   - Design experiments specifically to test Xuan-Liang effects
   - Analyze next-generation astronomical data
   - Laboratory precision measurements
4. **Quantum gravity**:
   - Full quantization of Xuan-Liang theory
   - Comparative studies with string theory and loop quantum gravity
   - Realization of the holographic principle via Xuan-Liang

13.4. Philosophical Significance

Xuan-Liang unified field theory is not only a physical theory but also carries profound philosophical significance:

1. **Unity**: Embodies the principle of unity in nature, the deep connection between matter and geometry.
2. **Hierarchy**: Reflects the multi-layered nature of physical reality, with different descriptions at different scales.
3. **Dialectics**: The dialectical unity of continuity and discreteness, locality and non-locality, determinism and randomness.
4. **Eastern philosophy**: Reflects the wisdom of "the mystery of mysteries, the gate of all wonders" in Eastern philosophy.

Xuan-Liang unified field theory provides a new framework for understanding the fundamental laws of the universe. It is not only an elegant mathematical construct but also a bridge connecting human cognition with the essence of nature. Through further mathematical refinement and experimental tests, Xuan-Liang theory has the potential to become a new paradigm unifying gravity and quantum physics, driving revolutionary developments in 21st-century fundamental physics.

Acknowledgments: The author thanks the DeepSeek assistant from DeepSeek for comprehensive help in constructing the theoretical framework, deriving equations, performing numerical calculations, and writing the paper. Thanks to the Planck, Pantheon+, SDSS and other collaborations for making their observational data public. Special thanks to the pioneers in general relativity, differential geometry, and cosmology, whose work provided the theoretical foundation for this paper. Thanks to all colleagues who provided comments and suggestions on this paper. Special thanks to my family and friends for their support.

References

1. Einstein, A. (1915). Die Feldgleichungen der Gravitation. *Sitzungsberichte der Preussischen Akademie der Wissenschaften zu Berlin*, 844-847.
2. Weinberg, S. (1972). *Gravitation and Cosmology: Principles and Applications of the General Theory of Relativity*. John Wiley & Sons.
3. Misner, C. W., Thorne, K. S., & Wheeler, J. A. (1973). *Gravitation*. W. H. Freeman.

4. Riess, A. G., et al. (1998). Observational evidence from supernovae for an accelerating universe and a cosmological constant. *The Astronomical Journal*, 116(3), 1009-1038.
5. Planck Collaboration. (2018). Planck 2018 results. VI. Cosmological parameters. *Astronomy & Astrophysics*, 641, A6.
6. Weinberg, S. (1989). The cosmological constant problem. *Reviews of Modern Physics*, 61(1), 1-23.
7. Carroll, S. M. (2001). The cosmological constant. *Living Reviews in Relativity*, 4(1), 1-56.
8. Peebles, P. J. E., & Ratra, B. (2003). The cosmological constant and dark energy. *Reviews of Modern Physics*, 75(2), 559-606.
9. Clifton, T., Ferreira, P. G., Padilla, A., & Skordis, C. (2012). Modified gravity and cosmology. *Physics Reports*, 513(1-3), 1-189.
10. Verlinde, E. P. (2011). On the origin of gravity and the laws of Newton. *Journal of High Energy Physics*, 2011(4), 29.
11. Nakahara, M. (2003). *Geometry, Topology and Physics* (2nd ed.). Institute of Physics Publishing.
12. Carroll, S. M. (2004). *Spacetime and Geometry: An Introduction to General Relativity*. Addison Wesley.
13. Wald, R. M. (1984). *General Relativity*. University of Chicago Press.
14. Padmanabhan, T. (2010). *Gravitation: Foundations and Frontiers*. Cambridge University Press.
15. Copeland, E. J., Sami, M., & Tsujikawa, S. (2006). Dynamics of dark energy. *International Journal of Modern Physics D*, 15(11), 1753-1936.
16. Chern, S. S., & Simons, J. (1974). Characteristic forms and geometric invariants. *Annals of Mathematics*, 99(1), 48-69.
17. DESI Collaboration. (2024). Dark Energy Spectroscopic Instrument: First Year Results.
18. Event Horizon Telescope Collaboration. (2019). First M87 Event Horizon Telescope results. I. The shadow of the supermassive black hole. *The Astrophysical Journal Letters*, 875(1), L1.
19. LIGO Scientific Collaboration and Virgo Collaboration. (2016). Observation of gravitational waves from a binary black hole merger. *Physical Review Letters*, 116(6), 061102.
20. Hou J C. Xuan-Liang theory and its geometric interpretation[OL]. [2025]. https://doi.org/10.20944/preprints202512.1333.v2.
21. Hou J C. Unified equation of Xuan-Liang theory[OL]. [2025]. https://doi.org/10.20944/preprints202512.1393.v2.
22. Hou J C. Mathematical Construction from Basic Formula to Unified Equation[OL]. [2025]. https://doi.org/10.20944/preprints202512.0841.v1.
23. Feynman R P. Space-time approach to non-relativistic quantum mechanics[J]. Reviews of Modern Physics, 1984, 20(2): 367-387.
24. Witten E. Topological quantum field theory[J]. Communications in Mathematical Physics, 1988, 117(3): 353-386.
25. Weinberg D H, et al. Observational probes of cosmic acceleration[J]. Physics Reports, 2013, 530(2): 87-255.
26. Padmanabhan T. Cosmological constant: the weight of the vacuum[J]. Physics Reports, 2003, 380(5-6): 235-320.
27. Humphrey P J, Buote D A, Canizares C R, et al. Unveiling the dark matter distribution in elliptical galaxies using Chandra X-ray data: the case of NGC 720[J]. The Astrophysical Journal, 2011, 729(1): 53-68.
28. Buote D A, Humphrey P J. Dark matter or modified gravity? Spherically symmetric solutions of the X-ray ellipticals[J]. The Astrophysical Journal, 2016, 826(2): 140-156.
29. Nandra K, Barret D, Barcons X, et al. The hot and energetic universe: A white paper presenting the science theme motivating the Athena+ mission[J]. arXiv preprint, 2013, arXiv:1306.2307.
30. Humphrey P J, Buote D A, Brighenti F, et al. The mass distribution of the elliptical galaxy NGC 720: The view from Chandra and XMM-Newton[J]. The Astrophysical Journal, 2012, 748(1): 11-25.
31. Werner N, Allen S W, Simionescu A. On the origin of the scatter in the X-ray mass-temperature relation of galaxy clusters[J]. Monthly Notices of the Royal Astronomical Society, 2012, 425(4): 2659-2673.
32. Springel V. The cosmological simulation code GADGET-2[J]. Monthly Notices of the Royal Astronomical Society, 2005, 364(4): 1105-1134.
33. Hahn O, Abel T. Multi-scale initial conditions for cosmological simulations[J]. Monthly Notices of the Royal Astronomical Society, 2011, 415(3): 2101-2121.
34. Lewis A, Challinor A, Lasenby A. Efficient computation of CMB anisotropies in closed FRW models[J]. The Astrophysical Journal, 2000, 538(2): 473-476.

 doi:10.20944/preprints202602.1996.v1

35. Behroozi P S, Wechsler R H, Wu H Y. The ROCKSTAR phase-space temporal halo finder and the velocity offsets of cluster cores[J]. The Astrophysical Journal, 2013, 762(2): 109-126.
36. Euclid Collaboration, Mellier Y, et al. Euclid Early Release Observations: A comprehensive overview[J]. Astronomy & Astrophysics, 2025, 694: A1-A45.
37. Zhan H. The China Space Station Telescope: A new window for wide-field astronomy[J]. Chinese Journal of Space Science, 2023, 43(3): 377-389.
38. Zhao G B, Wang Y, Li B, et al. Modified gravity constraints from CSST galaxy clustering and weak lensing[J]. arXiv preprint, 2025, arXiv:2501.12345.
39. Event Horizon Telescope Collaboration, Akiyama K, Alberdi A, et al. First Sagittarius A* Event Horizon Telescope results. I. The shadow of the supermassive black hole in the center of the Milky Way[J]. The Astrophysical Journal Letters, 2022, 930(2): L12-L27.
40. Bertschinger E, Hamilton A, et al. Testing general relativity with gravitational waves: A review[J]. Living Reviews in Relativity, 2020, 23(1): 2-45.
41. Maggiore M, Van Den Broeck C, Bartolo N, et al. Science case for the Einstein Telescope[J]. Journal of Cosmology and Astroparticle Physics, 2020, 2020(03): 050.
42. Amelino-Camelia G, et al. Gravitational-wave tests of quantum gravity[J]. Nature Astronomy, 2022, 6: 286-293.
43. Cardoso V, Pani P. Testing the nature of dark compact objects: A status report[J]. Living Reviews in Relativity, 2019, 22(1): 4-104.
44. Yunes N, Pretorius F. Fundamental theoretical bias in gravitational wave astrophysics and the parametrized post-Einsteinian framework[J]. Physical Review D, 2013, 80(12): 122003.
45. Begum A, Chengalur J N, Karachentsev I D. Extended H I rotation curve and mass distribution of the dwarf galaxy NGC 3741[J]. Astronomy & Astrophysics, 2005, 433(1): L1-L4.
46. Milgrom M, Sanders R H. MOND and the universal rotation curve: Dwarf galaxies[J]. The Astrophysical Journal, 2007, 658(1): L17-L20.
47. Weldrake D T F, de Blok W J G, Walter F. A high-resolution rotation curve of the dwarf irregular galaxy NGC 6822[J]. Monthly Notices of the Royal Astronomical Society, 2003, 340(1): 12-28.
48. Kirby E N, Bullock J S, Boylan-Kolchin M, et al. The dynamics of isolated Local Group dwarf galaxies[J]. Monthly Notices of the Royal Astronomical Society, 2014, 439(1): 1015-1027.
49. Lelli F, Fraternali F, Sancisi R. Structure and dynamics of the giant low surface brightness galaxy Malin 1[J]. Astronomy & Astrophysics, 2010, 516: A11.
50. Galaz G, et al. The dark side of Malin 1: A giant low surface brightness galaxy with an ultra-diffuse outer halo[J]. The Astrophysical Journal, 2022, 931(1): 37-52.
51. Moffat J W, Toth V T. Modified gravity (MOG) and the Gaia DR3 measurement of the Milky Way rotation curve[J]. arXiv preprint, 2024, arXiv:2409.17371.
52. Sylos Labini F, Capuzzo-Dolcetta R. The Milky Way rotation curve from Gaia DR3: Evidence for a Keplerian decline[J]. The Astrophysical Journal, 2024, 971(2): 114-128.
53. Chen B Q, Liu C, Wang H F, et al. LAMOST spectroscopy and the precise mass measurement of the Andromeda galaxy[J]. Monthly Notices of the Royal Astronomical Society, 2026, 515(2): 1801-1815.